

International comparison of activity measurements  
of a solution of  $^{109}\text{Cd}$  (March 1986)

by G. Ratel

September 1988

Bureau International des Poids et Mesures  
F-92310 SEVRES

International comparison of activity measurements  
of a solution of  $^{109}\text{Cd}$  (March 1986)

TABLE OF CONTENTS

	page
Abstract	1
1. Introduction	2
2. Description of the solution distributed and purity tests	3
3. Ionization-chamber measurements and adsorption tests	3
4. Source preparation	4
a) Sources for conversion-electron counting	
b) Sources for X- and/or $\gamma$ -ray counting	
5. Detectors for proportional and photon counting	5
a) Proportional counter (PC)	
b) Photon detector	
6. Counting data for the different methods	6
7. Activity and gamma-ray emission rate measurements	6
a) Measurements with pressurized proportional counters	
b) Measurements without a pressurized proportional counter	
8. Corrections used for calculating the results	9
9. Uncertainties	11
10. Final results	12
11. Determination of the total internal conversion coefficient $\alpha_t$	14
12. Conclusion	15
Acknowledgments	16
Table 1 - List of the participants	17
Table 2 - Mass measurements	18
Table 3 - Results of ionization-chamber measurements of activity and absorption tests for remaining activity	19
Table 4 - Source preparation for electron counting	20
Table 5 - Source preparation for $\gamma$ - and/or X-ray counting	22
Table 6 - Liquid-scintillation counting	23
Table 7 - $4\pi$ proportional counters used by the participants	24
Table 8 - Gamma- and X-ray detectors, dead times	26
Table 9 - Counting data for the different methods	27

	page
Table 10 - Formulae used for calculating the results	29
Table 11 - Corrections applied for calculating the results	35
Table 12 - Uncertainty components of the final result (in %)	38
Table 13 - Main uncertainty components of the final result	43
Table 14 - Final results	45
Table 15 - Mean values (in Bq mg <sup>-1</sup> ) for the activity concentration of <sup>109</sup> Cd, measured with a pressurized proportional counter	12
Table 16 - Mean values (in Bq mg <sup>-1</sup> ) for the activity concentration of <sup>109</sup> Cd, obtained by the "other methods"	12
Table 17 - Mean values (in Bq mg <sup>-1</sup> ) for the activity concentration of <sup>109</sup> Cd (any method), with and without the result of IFIN	13
Table 18 - Values of the conversion electron and of the $\gamma$ -ray emission rates obtained by performing the <sup>109</sup> Cd activity measurements	47
Table 19 - Values of the $\gamma$ -ray emission probabilities deduced from the conversion-electron and $\gamma$ -ray emission rates listed in Table 18	47
Figure 1 - Decay schemes of <sup>109</sup> Cd and <sup>109</sup> Pd	48
Figure 2.1 - Some typical spectra obtained by means of a pressurized proportional counter	49
Figure 2.2 - Typical photon spectra measured in order to obtain directly the 88 keV photon-emission rate	51
Figure 2.3 - X-ray spectrum measured by means of a well-type NaI(Tl) detector surrounding the pressurized proportional counter (PTB). Low-energy response of the ion chamber used by NPL to determine the 88 keV photon-emission rate	51
Figure 3 - Typical conversion-electron spectra obtained by means of the liquid-scintillation method.	52
Figure 4 - Typical spectra obtained by AECL and NBS when standardizing a <sup>109</sup> Pd solution	53
Figure 5 - Typical curves with the 4 $\pi$ e-X coincidence method used by ETL	54
Figure 6 - Typical spectrum from <sup>109</sup> Cd obtained by means of a 4 $\pi$ CsI(Tl) sandwich spectrometer	55
Figure 7 - Results of the <sup>109</sup> Cd comparison	56
References	57

Abstract

Eighteen laboratories have taken part in an international comparison of activity measurements of a solution of  $^{109}\text{Cd}$  organized by the Bureau International des Poids et Mesures. The main features of the various methods and detectors used by the participants are listed. Most of the laboratories employed only one method, but some (5) used two methods and others (2) even three. The final results and their uncertainties are presented in several tables, and on a graph where they are compared with a value obtained in the framework of the International Reference System. The total range of the results is 2.6 %. A weighted mean based on seventeen values of  $(5\,992 \pm 7)$  Bq  $\text{mg}^{-1}$ , and an unweighted one of  $(6\,001 \pm 15)$  Bq  $\text{mg}^{-1}$ , have been determined. The stated uncertainties may include a possible real discrepancy between two groups of activity concentrations obtained by different methods. The values resulting from the use of a pressurized proportional counter and those obtained by means of the  $4\pi(\text{LS})\text{ce}+4\pi\text{NaI}(\text{Tl})\gamma$  method and with a  $4\pi\text{CsI}(\text{Tl})$  spectrometer are significantly lower and less scattered than the values obtained by all the other methods. A new value for the  $\gamma$ -ray emission probability  $P_\gamma$  and for the total conversion coefficient was deduced from the measurements of nine laboratories. The weighted mean values  $P_\gamma = 0.036\,14 \pm 0.000\,12$  and  $\alpha_t = 26.67 \pm 0.09$  were obtained.

## 1. Introduction\*

$^{109}\text{Cd}$  is widely used in X-ray fluorescence excitation and provides one of the few useful efficiency-calibration points in the 88 keV energy region. Unfortunately, the activity of this nuclide is quite difficult to measure because of the long half life of the metastable state at 88 keV of  $^{109}\text{Ag}$  ( $T_{1/2} \approx 40$  s), which is reached only through electron capture.

Figure 1 shows the decay scheme of  $^{109}\text{Cd}$  and a list of some important related quantities. All the participants used the proposed half-life value of  $(462.6 \pm 0.4)$  d. The ground state of  $^{109}\text{Pd}$  is also indicated because it is relevant for one of the standardization methods described in this report. AECL used for  $^{109}\text{Pd}$  a half life of  $(13.405 \pm 0.007)$  h [1] and NBS took the value  $T_{1/2} = (13.404 \pm 0.008)$  h, which had been measured by D.D. Hoppes.

A trial comparison was organized by the Working Group for advising on future comparisons on behalf of Section II (Mesure des radionucléides) of the Comité Consultatif pour les Etalons de Mesure des Rayonnements Ionisants (CCEMRI). This exercise, which took place in December 1984 [2] among a limited number of participants (six), was considered to be a success. Therefore, it was decided, during the 8th meeting of Section II in 1985, to organize a full-scale comparison of this radionuclide. From the report quoted above [2] it can be seen that the use of a pressurized  $4\pi$  proportional counter (PPC) was preferred by most of the participating laboratories, but some other methods were also used. According to reference [2] five laboratories measured the activity concentration of the  $^{109}\text{Cd}$  solution by means of only one method (two of them also determined the  $\gamma$ -ray emission rate) and one laboratory used three methods.

As could be noted in previous comparisons, the national laboratories have again manifested a great interest in these measurements. Eighteen laboratories (listed in Table 1) participated and submitted their results.

The details of the organization were explained in a circular letter dated 12 February 1986 which was accompanied by a reporting form based on previous experience and adapted to the case of  $^{109}\text{Cd}$ . The chosen reference date was 1986-03-01, 00 h UT. Most of the filled-in forms reached BIPM by the end of June 1986; the last one arrived at the end of August. A preliminary report [3] presenting a summary of the information contained in the forms was issued in December 1986.

---

\* As this work is the first detailed report on an international comparison that has been written after the retirement of Dr. A. Rytz, we would like to dedicate it to him, although we doubt that it will match his high standards.

## 2. Description of the solution distributed and purity tests

At the 1985 meeting of Section II OMH offered to dilute and bottle the  $^{109}\text{Cd}$  solution supplied by NAC. All ampoules were sent on 27 January 1986 to LMRI who proceeded to the dispatching to the participating laboratories. Each participant (Table 1) received a flame-sealed NBS-type ampoule containing about 3.6 g of solution. The exact masses were communicated to the laboratories and are indicated in Table 2. The BIPM received two ampoules; one of them (ampoule number OMH-7581) was for the International Reference System for activity measurements of  $\gamma$ -ray-emitting nuclides (SIR).

The number of shipped ampoules was 21. Three laboratories decided not to participate after reception of their ampoule (two of them without notice).

The distributed solution had a nominal radioactivity concentration of  $6.0 \text{ MBq}\cdot\text{g}^{-1}$ , diluted in an aqueous solution of  $0.1 \text{ mol HCl per dm}^3$  with  $20 \mu\text{g}$  of  $\text{CdCl}_2$  per gram of solution.

### Purity tests

At the request of BIPM, IER performed, in October 1985, purity tests by  $\gamma$ -ray spectroscopy on a small part of the  $^{109}\text{Cd}$  solution prepared for the comparison. Similarly, LMRI carried out purity tests after receiving the ampoules. The results in percent of  $^{109}\text{Cd}$  activity and given at the reference date are listed below:

Laboratory	$^{65}\text{Zn}$	Impurity $^{110}\text{Ag}^{\text{m}}$	
IER	$(1.4 \pm 0.3) 10^{-6}$	$(3.2 \pm 0.7) 10^{-6}$	$T_{1/2} (^{65}\text{Zn}) = 243.9 \text{ d}$
LMRI	not detected	$(4.1 \pm 0.8) 10^{-6}$	$T_{1/2} (^{110}\text{Ag}^{\text{m}}) = 249.8 \text{ d}$

Apart from this, no other  $\gamma$ -ray-emitting impurity was detected in the  $^{109}\text{Cd}$  solution. The measurements were carried out by means of a Ge(Li) detector at LMRI and a pure Ge detector in the case of IER.

## 3. Ionization chamber measurements and adsorption tests

The ionization chamber measurements were carried out by nine laboratories before opening the ampoules and by seven after transferring and weighing the solution. The results of these measurements are in quite good agreement. After the ampoule had been emptied it was rinsed twice with distilled water. The remaining activity gave a measure of the adsorption on the ampoule walls which appeared to be smaller than  $3\cdot 10^{-5}$ .

NPL quoted a value which was ten times higher. BIPM noticed that after two rinsings no further activity could be detected in the empty ampoule. NBS did not perform these measurements because of their previous experience which indicated that a solution of  $^{109}\text{Cd}$  with  $20 \mu\text{g g}^{-1}$  of carrier in  $0.1 \text{ mol/l HCl}$  is stable for long periods of time. The results of mass measurements are presented in Table 2. From Table 3 it can be seen that adsorption tests were made by means of  $\gamma$ -ray spectrometry.

#### 4. Source preparation

In view of the two different measuring methods applied, this paragraph is divided into two parts: one is devoted to sources for electron counting and the other to sources for X- and/or  $\gamma$ -ray counting.

##### a) Sources for conversion-electron counting

Almost all sources were made from a diluted solution. KSRI alone used an undiluted solution for some of its sources. The dilution factors ranged from 1 (KSRI) to 301.6 (LMRI). NPL made a dilution in order to reduce the X-X summing. The sources were sandwiched by ETL and IFIN to eliminate the effects of Auger electrons. In most cases they were deposited on to gold-coated VYNS films. The range of the source masses was about the same for all laboratories, except for AECL which used very light sources to get good efficiencies for L-Auger electrons, the energy of which is about 3 keV. Other details can be found in Table 4.

##### b) Sources for X- and/or $\gamma$ -ray counting

Five laboratories (IFIN, KSRI, LMRI, PTB and UVVVR) used the same dilution as for the conversion-electron sources. KSRI used only sources obtained from the undiluted solutions. UVVVR sandwiched the sources with polyethylene foils. Further information is given in Table 5.

Details about source preparation for liquid-scintillation counting (LS) can be found in Table 6. Only five laboratories employed this method to determine the activity of the  $^{109}\text{Cd}$  solution. Three participants (IEA, NBS and NIM) also determined the activity by means of other techniques. NAC applied liquid-scintillation counting in two different ways. For IER it was the only method tested. All measurements were done with a solution diluted with  $\text{CdCl}_2$  and  $0.1 \text{ mol/l HCl}$ . NBS added diethylhexylphosphoric acid to chelate the radiocadmium. NIM used, in addition, a solution of toluene and alcohol. All vessels were made of glass, except in the case of IEA which used polyethylene vials. NBS studied very carefully the influence of the vial diameter on the value of the conversion-electron emission rate; the best results were obtained with a 3 ml vial inserted in a large cylinder filled with liquid.

Details on the sources necessary for the triple-to-double coincidence ratio method [4] used by IEA can be found in Table 6.

## 5. Detectors for proportional and photon counting

The major data concerning the detectors are listed in Tables 7 and 8. We can make the following remarks.

### a) Proportional counter (PC)

Fourteen laboratories used a proportional counter. Three of these instruments were operated at normal pressure to detect conversion electrons and low-energy L-Auger electrons (AECL), and two were connected with one or two photon detectors to permit  $4\pi e$ -X coincidence measurements (ETL [5], IFIN and AECL [6]) or the standardization of  $^{109}\text{Pd}$  alone for AECL [7]. All proportional counters were of the gas-flow type (except that of CBNM), filled with the same gas mixture (Ar +  $\text{CH}_4$  in the proportion 9 to 1) when they were pressurized, and with pure methane in the other case. All laboratories using a pressurized proportional counter to determine the conversion electron rate set a starting point for the tail extrapolation between 30 and 40 keV. For most of them the dead time applied was between 2 and 4  $\mu\text{s}$ . PTB and UVVVR worked with dead times of 5 and 6  $\mu\text{s}$ , respectively. BIPM and NPL chose a somewhat longer dead time of 15  $\mu\text{s}$ . In addition, BIPM assumed a first dead time of extended type (2.5  $\mu\text{s}$ ). It was determined by iteration [8] and supposed to be due to the detector and electronic chain.

### b) Photon detector

$\text{NaI(Tl)}$  crystals were used most often as scintillation detectors. Three laboratories (IER, LMRI and NBS) used a well-type  $\text{NaI(Tl)}$  crystal. CBNM and NAC preferred two  $\text{CsI(Tl)}$  crystals between which the source was sandwiched and one  $\text{CaF}_2(\text{Eu})$  crystal, respectively. Except for AECL, ETL and IEA, the solid angle was close to  $4\pi$  sr.

In the semiconductor category four laboratories made use of  $\text{Ge(Li)}$  detectors and three of high-purity Ge detectors. The volume of all semiconductor detectors ranged between 50 and 127  $\text{cm}^3$ . KSRI alone used a rather small detector. All entrance windows were protected with a foil of Be or Al. IMM used for this purpose two layers, of Al and Teflon (PTFE) respectively. Four laboratories used live-time measurements. PTB used a large (15.2 cm x 15.2 cm) well-type NaI detector housing the cylindrical proportional counter to measure the K X rays and used them as gate signals for a linear gate isolating the K-conversion electron spectrum from the pulse-height spectrum of the proportional counter.

Further data concerning the  $\gamma$ - and/or X-ray counting are listed in Table 8.

## 6. Counting data for the different methods

The counting data corresponding to the different measuring instruments are compiled in Table 9.

For PPC measurements we notice that a statistical precision better than 0.1 % was obtained in all cases with times shorter than 3 000 s. Most laboratories achieved a much better statistical precision in one run.

For Ge(Li) counting, all laboratories operated with small count rates from  $0.5 \text{ s}^{-1}$  (IFIN) to  $120 \text{ s}^{-1}$  (IMM). Typical count rates for NaI(Tl),  $\text{CaF}_2(\text{Eu})$  and pure Ge, were in general higher and approximately the same for each. KSRI worked with a small count rate ( $9 \text{ s}^{-1}$ ) for its pure Ge detector. On the contrary, count rates for the CsI(Tl) (CBNM) have about the same value as for the pressurized proportional counters.

## 7. Activity and gamma-ray emission rate measurements

At this stage of the presentation of the results it is important to give some details about the different methods used by the laboratories to measure the activity.

In fact, there are two groups of laboratories:

- those which carried out measurements to count the conversion-electron emission rate by means of a pressurized proportional counter and determined (or did not) the  $\gamma$ -ray emission rate using a scintillation counter or a semiconductor detector;
- those which used a variety of other methods.

This separation into two groups of methods is only an attempt at simplifying the presentation of the results.

### a) Measurements with pressurized proportional counters

Eleven laboratories (CBNM, BIPM, IMM, IPEN, KSRI, LMRI, NIM, NPL, OMH, PTB and UVVVR) used a pressurized proportional counter in the conversion-electron channel. Four of them (BIPM, IMM, IPEN and NIM) calculated the activity concentration of the solution of  $^{109}\text{Cd}$  directly from the conversion-electron emission rate by multiplying it with a normalizing constant which is a function of the  $\gamma$  efficiency of the  $\beta$  detector  $\varepsilon_{\beta\gamma}$  and of the tabulated total internal conversion coefficient  $\alpha_t$  ( $\alpha_t = 26.4 \pm 0.5$ ). Further details on this method are given for instance by M.E.C. Troughton [9]. As  $\alpha_t$  is rather poorly known at present, it also contributes to the uncertainty of the final results. This is the reason why the participants were asked to measure independently the  $\gamma$ -ray emission rate. In fact,  $\alpha_t$  does not seriously degrade the accuracy of the activity measurements, as can be seen in Table 10.

Seven other laboratories succeeded in measuring the  $\gamma$ -ray emission rate by means of scintillation detectors: NaI(Tl) at LMRI and UVVVR, CsI(Tl) at CBNM or Ge semiconductor detectors at KSRI, OMH and PTB. NPL deduced the  $\gamma$ -ray emission rate from measurements with a high-precision ionization chamber.

The main problem for this method consists in setting the discrimination threshold at the appropriate place for reducing the contribution of X rays and Auger electrons in the conversion-electron spectrum. A correction has to be applied in order to take account of the conversion electrons below the threshold and to eliminate the contributions of the X rays and Auger electrons to the spectrum above the threshold.

Some typical spectra are shown in Figure 2.

b) Measurements without a pressurized proportional counter

In this group we have collected all the other techniques used to determine the activity concentration of the  $^{109}\text{Cd}$  solution.

Five laboratories applied a liquid-scintillation counting technique (IEA, IER, NAC, NBS and NIM) but in three different manners.

IEA and NAC used the  $4\pi(\text{LS})\text{e-X}$  coincidence method which measures the disintegration rate of the solution, but depends on some decay-scheme parameters. The formulae applied for the calculation are presented in Table 10. Both laboratories used the same values for  $\alpha_t$  and  $\alpha_K$  [10]. Examples of spectra are shown in Figure 3.

IER, NBS and NIM measured the conversion electron rate by means of a liquid-scintillation method (without coincidence). In order to obtain the total concentration activity, IER and NBS measured the  $\gamma$ -ray emission of the diluted solution with a high-efficiency, well-type NaI(Tl) counter and they added the two results. NIM determined the total activity concentration by means of the same method as BIPM, IMM and IPEN.

NAC also used the liquid-scintillation method and made  $4\pi\text{e-}4\pi\text{e}$  coincidence counting between signals collected by two phototubes. The variation of the counting efficiency in one of the channels was obtained by a threshold discrimination. Eleven bias levels were set for each source and the corresponding coincidences were counted simultaneously. The efficiencies ranged from 0.21 to 0.85.

NBS employed the liquid-scintillation method in order to measure the activity of a  $^{109}\text{Pd}$  sample. The activity concentration of the  $^{109}\text{Cd}$  solution was obtained from a comparison of the 88 keV  $\gamma$ -ray rates of the two solutions by means of a NaI(Tl) detector and also of a Ge(Li) spectrometer.

AECL performed the measurements in the same way, but instead of the liquid-scintillation system they used a gas-flow proportional counter.

They made the  $\gamma$ -ray rate comparison only with a Ge(Li) detector. Details on their formulae are given in Table 10. Figure 4 shows some of the spectra obtained at NBS and AECL.

ETL measured  $4\pi e$ -X coincidences using a proportional counter for the electron channel and a NaI(Tl) detector to detect the 22 keV X rays [5]. The conversion-electron count rate was derived by extrapolating a plot of count rate vs. counting efficiency. A typical  $\gamma$ -ray spectrum from  $^{109}\text{Cd}$  and a curve showing the behaviour of the  $\beta$  count rate vs. the efficiency  $(\epsilon_{ce})_K$  can be found in Figure 5.

A similar procedure was also used by AECL, with the conversion electrons and Auger electrons detected by means of a gas-flow proportional counter. An extrapolation was necessary to obtain the desired  $^{109}\text{Cd}$  activity concentration. Some of the needed formulae are listed in Table 10.

CBNM used a  $4\pi\text{CsI(Tl)}$  spectrometer in order to obtain the activity concentration of the  $^{109}\text{Cd}$  solution from the sum of the conversion electrons and  $\gamma$  rays. Spectrum measurements and integral counting were done concurrently. When required, an electronic threshold was set in the counting chain and the corresponding channel number in the spectrum determined. This approach permits a more reliable dead-time correction than does a mere measurement of the spectrum. An extrapolation of the low-energy tail of the spectrum is also necessary. Typical spectra are shown on Figure 6.

IEA used the triple-to-double coincidence ratio method, which is explained in ref. [4]. The principle is as follows. A triple liquid-scintillation detector gives two outputs: one is a triple coincidence signal and the other one the logic sum of double coincidences. From these data a triple-to-double coincidence ratio (TDCR) can be calculated.

UVVVR tried also to measure the activity concentration of the  $^{109}\text{Cd}$  solution by means of the measurement of the X-ray or  $\gamma$ -ray emission rates or the  $\gamma$ -ray emission rate with a NaI(Tl) detector. These two methods imply the use of the efficiency curve of the scintillation detector and are expected to measure an event which occurs with a small and uncertain probability ( $P_\gamma \approx 0.037$ ). Therefore, they cannot lead to a very precise determination. The formulae used for the calculation of the activity are given in Table 10.

IFIN used a  $4\pi$  unpressurized proportional counter and a NaI(Tl) detector in order to form coincidences between the internal conversion electrons and the K X rays. To eliminate the Auger electrons it was necessary to put on each side of the sources a metallized film of  $600 \mu\text{g cm}^{-2}$ . The measurement of the  $\gamma$ -ray emission rate was done by means of a Ge(Li) detector. To calibrate the detector, some known  $\gamma$ -ray emission probabilities were used. The remark made for UVVVR applies here also. Table 10 contains the formulae used in order to obtain the  $^{109}\text{Cd}$  activity concentration.

## 8. Corrections used for calculating the results

A summary of the corrections made by the different laboratories for calculating the results is given in Table 11. For a large part the corrections depend on the measuring method, but all count rates were corrected for background, dead times and radioactive decay during the measurements.

AECL made the radioactive-decay correction from the effective midpoint of the counting period. It was also corrected for delay mismatch, accidental coincidences and pile-up. For obtaining the activity concentration of the  $^{109}\text{Cd}$  solution, this laboratory applied to both methods an extrapolation by least-squares.

In fact, all laboratories using a pressurized proportional counter corrected for the largest contribution correlated with this experimental method: they had to estimate the form of the tail of the spectrum under the K-X and K-Auger electron peak. In addition, they corrected for pile-up, self and foil absorption, and if they did not measure directly the 88 keV  $\gamma$ -ray emission, they had to estimate its contribution to the spectrum.

BIPM determined experimentally the value of the  $\gamma$  efficiency of the  $\beta$  detector and found that  $\varepsilon_{\beta\gamma}$  always remains below 0.5 %. IPEN used 0.3 % and NIM quite a larger value (1 %). A correction was also applied for radioactive decay from the beginning of the counting time.

In the case of the measurements with a pressurized proportional counter, CBNM used for the correction the calculations of Bambynek [11] but, as mentioned by Reher et al. [10], because of the small  $\gamma$ -ray emission probability, the contribution of the  $\gamma$  rays of 88 keV to the conversion electron peaks remains rather small. Due to this fact, CBNM did not correct for this contribution, as did the other laboratories, but decided to include it in the uncertainty of the final result. When CBNM worked with its windowless  $4\pi\text{CsI(Tl)}$  sandwich spectrometer, the conversion electrons and  $\gamma$  rays were counted at the same time and summed automatically. A low-tail correction by exponential extrapolation to zero energy was applied.

LMRI made an extrapolation for the shape of the spectrum from 0 to 35 keV in the form  $N = A e^{-BC}$ , where  $N$  is the count rate,  $C$  the channel number, and  $A$  and  $B$  two adjustable parameters, whereas BIPM used a linear extrapolation.

To take into account the tail of K, L, M conversion electrons which are below the discrimination threshold, UVVVR measured the count rate dependency on the pressure. The count rate was saturated if the pressure was equal to 0.9 MPa. For a working pressure of 0.5 MPa the correction was found to be  $(1.7 \pm 0.2)$  %.

KSRI used for conversion-electron measurements a diluted solution in order to avoid peak-summing, pile-up and dead-time effects. For measuring the  $\gamma$ -ray emission, they used an undiluted solution because of its low intensity.

NPL determined the number of detected 88 keV  $\gamma$  rays in the pressurized proportional counter by means of the relation  $N_{\gamma\text{PPC}} = N_{\gamma} \epsilon_{\gamma}$ , where  $N_{\gamma}$  was directly measured and  $\epsilon_{\gamma}$  was calculated and found to be  $0.008 \pm 0.002$  at 0.5 MPa. This laboratory also used a dilution giving a count rate lower than or equal to  $1\ 000\ \text{s}^{-1}$  in order to reduce X-X summing.

PTB estimated the fraction of the conversion electrons below 30 keV by extrapolating the shape of the K conversion electron to zero energy. This shape was taken from the proportional-counter spectrum gated by pulses from K X rays detected in a well-type NaI(Tl) detector surrounding the proportional counter. In order to correct the results given by the  $4\pi\text{CsI(Tl)}$  spectrometer, CBNM made two linear extrapolations which agreed very well: one for the low-energy side of the conversion-electron peak down to zero energy, and the other for the high-energy side of the Auger electrons and K X rays, with small corrections for pile-up, up to 50 keV.

ETL made corrections for the random coincidences according to Campion's formula. A small correction for the sensitivity of the  $4\pi\beta$  counter to the X rays was also applied and can be found in Table 10.

IEA applied some corrections for its TDCR method [4] which are listed in Table 11. For the  $4\pi(\text{LS})\text{e-X}$  coincidence, an extrapolation was used to obtain the activity concentration.

IER corrected for a mass-dependent loss of efficiency and extrapolated the tails of the conversion-electron spectrum below the threshold and those of the X-ray spectrum above the threshold.

IFIN corrected for the resolving time of its electronic instruments.

NAC corrected for their coincidence resolving time ( $0.57\ \mu\text{s}$ ) and for satellite pulses. The experimental conversion-electron efficiency curves determined by the two methods used were fitted by a second-order polynomial.

When measuring the activity concentration by means of the  $4\pi(\text{LS})\text{ce}+4\pi\text{NaI(Tl)}\gamma$  method, NBS applied a small correction for the  $\gamma$ -ray contribution, based on a value taken from the literature for the total internal conversion coefficient  $\alpha_t$  and a calculated efficiency, as did NPL. During the standardization of  $^{109}\text{Cd}$  by comparison of the activity of a  $^{109}\text{Pd}$  sample, NBS made corrections for accidental coincidences between the 22.1 keV and the 88 keV photons by means of an extrapolation of the count rate for zero mass of the  $^{109}\text{Cd}$  solution.

The  $\gamma$ -ray results were also corrected for the photoelectric absorption in the liner, for solid angle, for the count rate below a 39 keV threshold (photoelectron escape, Compton backscatter and Bremsstrahlung pulses in the NaI(Tl) crystal), for photoelectric absorption in the mylar foil and for backscatter from the shield, phototube and liner.

NIM applied to the liquid-scintillation counting the same corrections as for the measurements with a pressurized proportional counter already mentioned above. However, a value of 0.001 7 for the  $\gamma$  efficiency of the  $\beta$  detector was used.

The corrections for the other two methods used by UVVVR are listed in Table 11.

## 9. Uncertainties

As in previous comparisons, the participants assessed values for the uncertainty components and indicated how they were obtained.

There are two kinds of uncertainty components. Some are common to all methods, such as those due to counting statistics, weighing, wall adsorption or impurities. Others, which are more specific of the method used, are, for instance, uncertainties due to  $\alpha_t$ ,  $\epsilon_{\beta\gamma}$ , extrapolations or dilution. For a more complete listing see Table 12.

It is interesting to know the origin of the main uncertainty contributions for the various laboratories. From Table 13 it can be seen that the laboratories using a  $4\pi$  pressurized proportional counter assessed smaller total uncertainties for their measurements. The extrapolations of the spectrum in the region below the threshold to take into account all conversion electrons, and above it to eliminate the contributions of Auger electrons and X rays, seem to be the most important sources of uncertainty for this method.

It is evident that the method which measures directly the activity of the  $^{109}\text{Cd}$  solution from the photon emission gives less precise results because of the small value of the photon-emission probability.

All the uncertainty components are considered as approximations of the corresponding standard deviations and are added in quadrature [13]. Only two laboratories have given their uncertainties at a 99 % confidence level; these values have been reduced accordingly.

## 10. Final results

The values of the activity concentration and their combined uncertainties, both taken at the reference date (1986-03-01, 00 h UT), are given in Table 14 and shown in Figure 7.

With the exception of the value determined by UVVVR, all the results obtained by means of a pressurized proportional counter are very close to each other. The total spread of all the measurements (without IFIN) is 2.6 %. The weighted and unweighted mean values of the results obtained with a pressurised proportional counter are given in Table 15.

The mean value  $\bar{x}$  and its standard deviation  $s(\bar{x})$  have been evaluated by means of the well-known formulae (for  $n$  data  $x_i \pm s_i$ ):

$$\bar{x} = \frac{\sum_{i=1}^n g_i x_i}{\sum_{i=1}^n g_i} \quad \text{and}$$

$$s^2(\bar{x}) = \frac{\sum_{i=1}^n g_i (x_i - \bar{x})^2}{(n - 1) \sum_{i=1}^n g_i},$$

where  $g_i = 1/s_i^2$  when weights are applied; otherwise  $g_i = 1$ .

Table 15 - Mean values (in Bq mg<sup>-1</sup>) for the activity concentration of <sup>109</sup>Cd, measured with a pressurized proportional counter

	mean value (all labs)	mean value (without UVVVR)
weighted	5 983 ± 11	5 973 ± 4
unweighted	5 995 ± 12	5 984 ± 5

Similarly, it is possible to calculate weighted and unweighted means of the results obtained with other methods (i.e. excluding pressurized proportional counters), as shown in Table 16.

Table 16 - Mean values (in Bq mg<sup>-1</sup>) for the activity concentration of <sup>109</sup>Cd, obtained by the "other methods"

	mean value (all labs)	mean value (without IFIN)
weighted	6 018 ± 12	6 015 ± 7
unweighted	6 034 ± 30	6 005 ± 8

For IEA only the mean value  $A(^{109}\text{Cd}) = (6\ 019 \pm 18)$  Bq  $\text{mg}^{-1}$  of the two results obtained with the TDCR method (and two different dilutions), as suggested by this laboratory, has been taken into account. Likewise, for IFIN only the mean value  $A(^{109}\text{Cd}) = (6\ 440 \pm 70)$  Bq  $\text{mg}^{-1}$  has been used.

From Tables 15 and 16 it can be seen that the two groups of methods for measuring the activity concentration give significantly different mean values. The discrepancy is more marked when the weighted mean values are taken.

When all results are considered, the mean values are as given in Table 17.

Table 17 - Mean values (in Bq  $\text{mg}^{-1}$ ) for the activity concentration of  $^{109}\text{Cd}$  (any method), with and without the result of IFIN

	mean value (all labs)	mean value (without IFIN)
weighted	5 993 $\pm$ 8	5 992 $\pm$ 7
unweighted	6 017 $\pm$ 18	6 001 $\pm$ 7

For IEA and IFIN the same remarks as for Table 16 can be made.

In fact, the values obtained by means of the method in which the pressurized proportional counter has been replaced by a liquid scintillator (NBS, IER) or which employ a  $4\pi\text{CsI(Tl)}$  spectrometer (CBNM) could also be included in the first group, because the data are used in the same way. The values of NBS and IER are somewhat lower than the results previously mentioned for pressurized proportional counters, but still much closer to them than to those obtained by most of the other methods. The  $4\pi\text{CsI(Tl)}$  spectrometer and the pressurized proportional counters give similar results.

The final values given in Table 17 allow us to state that (ignoring the data of IFIN) they hardly depend on the chosen weighing procedure, which is a welcome feature. The results of IFIN differ from the other values (by 6.6 % for their lowest result); hence it is better to leave them aside. Indeed, as suggested recently by IFIN, a problem with the homogeneity of the solution received cannot be excluded. In spite of the quite small uncertainty (0.12 %) of the final mean value, we should not forget the conclusion to be drawn from Tables 15 and 16, namely, that in fact one averages over two "populations", the means of which might differ by as much as 0.7 %.

One may consider the results obtained by using a pressurized proportional counter to be the most reliable ones, as is evidenced by their smaller uncertainties and the fact that this method deals with the most frequent event occurring in the  $^{109}\text{Cd}$  decay. However, considering the care taken by the participating laboratories with the other methods,

there is no good reason to discard their results. Possibly, the relevant question is whether the small uncertainties assigned to the first method are realistic or whether a common correction has been neglected in the determination of the activity concentration.

Figure 7 also indicates the result obtained on the basis of the  $\gamma$ -ray measurements available from the International Reference System (SIR), namely  $A(^{109}\text{Cd}) = (5\,994 \pm 30) \text{ Bq mg}^{-1}$ . This value is in good agreement with all the (weighted and unweighted) values given in Tables 15 to 17.

From Figure 7 and Table 15 it can equally be seen that the value of UVVVR (for PPC) is about  $(2.0 \pm 0.2) \%$  higher than the mean of the other values based on the same method. UVVVR has therefore been asked to check its result carefully. Should it be withdrawn, then the observed discrepancy between different methods would increase.

#### 11. Determination of the total internal conversion coefficient $\alpha_t$

As suggested by Section II, nine laboratories (IER, IMM, KSRI, LMRI, NBS, NPL, OMH, PTB and UVVVR) determined the activity of the  $^{109}\text{Cd}$  solution by measuring independently both the conversion-electron and the  $\gamma$ -ray emission rates, and adding the results. In this way, it was not necessary to rely on a value taken from the literature for the total internal conversion coefficient  $\alpha_t$  or the  $\gamma$ -ray emission probability  $P_\gamma$ . In fact, it can be seen from Table 11 that these values have an uncertainty of more than 1 %.

The conversion-electron and the  $\gamma$ -ray emission rates obtained by all the laboratories which have performed these measurements are listed in Table 18. They show a spread of 2.6 % and 3.8 %, respectively.

From the experimental values contained in Table 18, it is easy to deduce values for  $P_\gamma$  and  $\alpha_t$  by means of the relations

$$P_\gamma = \frac{N_\gamma}{N_\gamma + N_{ce}} \quad (1)$$

and

$$P_\gamma = \frac{1}{1 + \alpha_t},$$

which is equivalent to

$$\alpha_t = \frac{1 - P_\gamma}{P_\gamma}. \quad (2)$$

The values of  $P_\gamma$  and their uncertainties are listed in Table 19. This allows us to calculate a weighted and an unweighted mean for the  $\gamma$ -ray emission probabilities designated as  $\bar{P}_\gamma$  and  $\bar{P}'_\gamma$ , respectively.

This leads to

$$\bar{P}_{\gamma} = 0.036\ 14 \pm 0.000\ 12 \quad (0.33 \%)$$

and

$$\bar{P}'_{\gamma} = 0.036\ 35 \pm 0.000\ 16 \quad (0.44 \%) ,$$

where the relative uncertainties are indicated in parentheses.

Equation (2) gives readily the two corresponding values for the total internal conversion coefficient (using a similar notation)

$$\bar{\alpha}_t = 26.67 \pm 0.09 \quad (0.34 \%)$$

and

$$\bar{\alpha}'_t = 26.51 \pm 0.11 \quad (0.45 \%) .$$

## 12. Conclusion

Various methods have been applied by the 18 participating laboratories in order to measure the activity concentration of  $^{109}\text{Cd}$ . Let us first look at the data obtained by means of a pressurized proportional counter: the uncertainties - provided that they have been realistically estimated - are quite small and all the values (except one) obtained for the activity concentration are in excellent mutual agreement.

Two methods, namely  $4\pi\text{CsI(Tl)}$  and  $4\pi(\text{LS})\text{ce}+4\pi\text{NaI(Tl)}\gamma$ , used by CBNM, IER and NBS, respectively, are very similar to the one considered in Section 7, in the data analysis, and give quite comparable results. However, the results of the remaining methods, although more scattered, should certainly not be ignored as the experiments have been performed equally carefully. On the other hand, the two values of IFIN are no doubt to be excluded. It should also be emphasized that the mere measurement of the photon emission of the  $^{109}\text{Cd}$  solution by means of a semiconductor or a scintillation counter, although quite simple to perform, is not the best way to determine the activity concentration of  $^{109}\text{Cd}$ , since it is based only on a small fraction of the total emitted radiation. In addition, the result of UVVVR, obtained with a pressurized proportional counter, may have to be checked, but even if its value should be changed, the main problem would remain, namely a small, but significant unexplained discrepancy between different methods. Only a new and careful look at all the methods used in the present comparison may possibly lead to the detection of a hitherto unsuspected error, the elimination of which could improve the overall agreement. Thus, the results of the present intercomparison may be considered as a hint to an unsolved problem and could encourage someone to perform a comparative study of the various methods used.

The new values for  $P_\gamma$  and  $\alpha_t$  deduced from the conversion electron and the  $\gamma$ -ray emission rates measured by ten participants, although somewhat higher, are of a much better precision than those published in the literature. This can be considered as an important improvement for these data.

#### Acknowledgments

We should like to thank all the participating laboratories for their great effort. To some of them BIPM is particularly indebted for the generous help without which it would not have been possible to carry out successfully this international comparison. Let us first mention NAC for supplying the  $^{109}\text{Cd}$  solution, then OMH for the preparation and bottling, and finally LMRI for the dispatching. We are also grateful to IER and LMRI for their careful execution of the purity tests.

The author of this report would also like to express his gratitude to Prof. A. Allisy for the permanent interest he has shown in this work and to Dr. J.W. Müller for many helpful and stimulating discussions. Furthermore, he is indebted to all the technicians of the Radionuclide group of BIPM for their untiring assistance. Last but not least he thanks Mrs. D. Müller for the careful typing and retyping of the text.

Table 1 - List of the participants

		<u>Names of the persons who carried out the measurements</u>
AECL	Atomic Energy of Canada Limited, Chalk River, Canada	R.H. Martin
BIEM	Bureau International des Poids et Mesures, Sèvres, France	P. Bréonce, C. Colas, G. Ratel
CBNM	Central Bureau for Nuclear Measurements, CEC-JRC, Geel, Belgium	D.F.G. Reher, B. Denecke
ETL	Electrotechnical Laboratory, Ibaraki, Japan	Y. Hino, Y. Kawada
IEA	Instytut Energii Atomowej, Swierk, Poland	R. Broda, A. Chyliński, K. Pochwalski, T. Radoszewski, T. Terlikowska-Drozdziel
IER	Institut d'Electrochimie et Radiochimie de l'EPFL, Lausanne, Switzerland	J.-J. Gostely
IFIN	Institutul de Fizika si Inginerie Nucleara, Bucuresti Magurele, Rumania	L. Grigorescu, M. Sahagia, R. Dimitrescu
IMM	Institut de Métrologie D.I. Mendéléev, Leningrad, USSR	A.A. Konstantinov, T.E. Sazonova, S.V. Sepman, A.I. Ivanov, G.A. Isaakyan
IPEN	Instituto de Pesquisas Energéticas e Nucleares São Paulo, Brazil	M.S. Dias, M.F. Koskinas, E. Pocobi
KSRI	Korea Standards Research Institute, Taejon, Korea	Tae Soon Park, Pil Jae Oh, Sun-Tae Hwang
IMRI	Laboratoire de Métrologie des Rayonnements Ionisants, Saclay, France	B. Chauvenet
NAC	National Accelerator Centre, Faure, South Africa	B.R.S Simpson, B.R. Meyer
NBS	National Bureau of Standards, Gaithersburg, USA	C. Ballaux, B.M. Coursey, D.D. Hoppes
NIM	National Institute of Metrology, Beijing, China	Li Fen, Wu X.Z., Li Zuo Qian
NPL	National Physical Laboratory, Teddington, UK	D.H. Woods, D. Smith
OMH	Országos Mérésügyi Hivatal, Budapest, Hungary	A. Szörényi, A. Zsinka, M. Csikós, Gy Horváth
PTB	Physikalisch-Technische Bundesanstalt, Braunschweig, FRG	E. Funck, U. Schöttzig
UVVU	Institute for research, production and application of radioisotopes, Prague, Czechoslovakia	J. Plčh, J. Šurán

Table 2 - Mass measurements

Laboratory	Ampoule number	Mass of solution (g)	
		indicated by OMH	determined by laboratory
AECL	OMH-7 565	3.603 5	
BIPM	OMH-7 573	3.605 6	3.591 2
CBNM	OMH-7 563	3.606 1	
ETL	OMH-7 572	3.603 2	
IEA	OMH-7 567	3.604 8	3.600 6
IER	OMH-7 560	3.605 5	3.584 9
IFIN	OMH-7 566	3.604 7	
IMM	OMH-7 570	3.604 4	
IPEN	OMH-7 568	3.602 8	
KSRI	OMH-7 569	3.604 3	
LMRI	OMH-7 561	3.603 7	3.603 1
NAC	OMH-7 574	3.602 8	3.593 6*
NBS	OMH-7 579	3.603 0	
NIM	OMH-7 571	3.602 9	2.693 236
NPL	OMH-7 575	3.605 4	3.593 3
OMH	OMH-7 557	3.606 0	3.598 8
PTB	OMH-7 576	3.605 1	3.605 3
UVVVR	OMH-7 577	3.605 0	

\* The empty ampoule (2 pieces) was re-weighed one month later and the mass of solution was found to be 3.602 3 g.

Table 3 - Results of ionization-chamber measurements of activity and adsorption tests for remaining activity

Laboratory	Activity concentration at reference date (kBq g <sup>-1</sup> )	Activity remaining in the "empty" ampoule after 2 rinsings with distilled water (Bq)	Measurement method used for adsorption tests	Number of additional rinsings	Final residual activity (Bq)
AECL	5 932 ± 24 o	560 ± 30	Ge-Li spectrometer	2	160 ± 30
BIPM	5 994 o 6 005 t	not detected	calibrated ionization chamber		
ETL		not detected	pressurized (1.0 MPa) 4π ionization chamber		
IEA		130	NaI(Tl) scintillation counter	1	120
IER	5 962 o 5 960 t	465	well-type 2" x 2" NaI detector		
IPEN		139	well-type NaI detector	2	18
LMRI	6 030 o		calibrated ionization chamber	1	
NAC	6 291 o 6 228 t	106 ± 70	NaI detector measuring 88 keV γ rays	3	56 ± 70
NIM	6 098 ± 58 o 6 013 ± 57 t		Liquid scintillation counting	1	111 ± 1
NPL	6 022 o 6 018 t	11 000	calibrated Ge detector	3 *	2 500
OMH	5 984 o 5 987 t	260 ± 20	calibrated Ge-Li spectrometer	2 **	200 ± 40
PTB	5 983 ± 20 o 5 971 ± 20 t	500 ± 20	Ge-Li detector		
UVVVR			calibrated well-type NaI(Tl)	3 + 2	185

\* Additional rinsing with a solution of 20 μg/g CdCl<sub>2</sub> in 0.1 M HCl

\*\* Additional rinsing done with a diluent

o before opening

t after transfer

Table 4 - Source preparation for electron counting

Laboratory	Diluent		Number of dilutions	Dilution factors	Source backing			Total mass ( $\mu\text{g cm}^{-2}$ )	Wetting or seeding agent	Drying	Special treatment	Range of source mass (mg)	Number of sources used
	$\text{CdCl}_2$ ( $\mu\text{g g}^{-1}$ of solution)	$\text{mol HCl/dm}^3$ of solution			Substrate metal coating	Number of films metal layers							
AECL	18	0.1	2	20.323 52.241	VYNS Au-Pd	1 or 2	0 a 1 or 2 b	20	Catanac SN	air 50 °C	-	0.36 to 0.86 1)	6 2)
BHM	20	0.1	1	34.172 4	VYNS Au	1	1 a 1 b	55 *	Ludox SM $10^{-4}$	air	-	10 to 70	28
CBM	20	0.1	5	39 to 217	VYNS Au	1	1 a 1 b	30 *	Catanac	air stream	-	20 to 58	10
ETL	20	0.1	2	6.152 3 5.651 2	VYNS Au	1	1 a 1 b	45 *	Cataloid SI-350 3)	4)	5)	8 to 19	dil. 1 22 dil. 2 17
IFIN	-	0.1	1	10.540	VYNS Au	6	3 a 3 b	1 200 *	no	ambient conditions	-	12 to 25 6)	6
IMM	-	0.1	3	11.252 20.320 29.799	X-ray film Au	1	1 a 1 b	30 *	Insulin + Catanac	infrared lamp in $\text{NH}_3$ atmosphere	-	4 to 20	10
IPEN	20	0.1	3	112.468 58.018 66.945	Collodion Au	1	0 a 1 b	30	Cyastat SN	warm $\text{N}_2$ stream	-	26 to 38	16
KSRI	20	0.1	2	1 7.244 4	Collodion Au	2	0 a 1 b	40 *	Ludox SM $15 \times 10^{-4}$	air	-	15 to 18	12
IMRI	20	0.1	1	301.556 ± 0.015	Cellulose Au	1	1 a 1 b	20 *		air	7)	11 to 26	10

Table 4 (cont'd)

Laboratory	Diluent		Number of dilutions	Dilution factors	Source backing			Total mass ( $\mu\text{g cm}^{-2}$ )	Wetting or seeding agent	Drying	Special treatment	Range of source mass (mg)	Number of sources used
	$\text{CdCl}_2$ ( $\mu\text{g g}^{-1}$ of solution)	mol HCl/dm <sup>3</sup> of solution			Substrate metal coating	Number of films	metal layers						
NIM	20	0.1	3	12.723 6	VYNS	2	1 a	20 *	$\text{SiO}_2$ Catanac	8)	-	12 to 25	30
				11.407 5	Au	1 b							
				1.361 8									
NPL	20 5	0.1 0.1	2	463.32	VYNS	1	1 a	50 *	50 $\mu\text{g g}^{-1}$ Catanac	air	-	17 to 59	14
				180.43	Au	1 b							
OMH	20	0.1	2	4.936 2 $\pm$ 0.000 5 60.033 $\pm$ 0.006	VYNS Au-Pd	1	1 a 1 b	30 + 5 *	Ludox + Teepol	infrared lamp	-	8 to 12	21
PTB	45 mg l <sup>-1</sup>	0.1	1	4.728 4	VYNS Au-Pd	1	1 a 1 b	55 *	Ludox SM 10 <sup>-4</sup>	air	-	10 to 11	7
UVVVR		0.1	2	29.927 7 27.682 8	VYNS Au	2	1 a 1 b	40 *	Insulin + Ludox + Aquadac	air normal temperature	-	20 to 40	11 11

a above b below

1) in terms of mass of the original solution

2) sources used for the  $4\pi$  Auger electron X-ray coincidence counting of  $^{109}\text{Cd}$

3) equivalent to Ludox SM30

4) drying in a desiccator with silicagel

5) in order to eliminate the effects due to L-Auger electrons and also to adjust the counting efficiency of conversion electrons, sources were sandwiched with aluminum-coated polystyrene film ( $0.5 \text{ mg cm}^{-2}$  to  $1.5 \text{ mg cm}^{-2}$ ) or thin aluminum foil ( $1.5 \text{ mg cm}^{-2}$  to  $5 \text{ mg cm}^{-2}$ )

6)  $600 \mu\text{g cm}^{-2}$  on both sides are necessary to stop Auger electrons

7) electro spraying of resins

8) air with  $\text{H}_2\text{O}$  and  $\text{C}_2\text{H}_5\text{OH}$

\* drop was dispensed onto metal

Table 5 - Source preparation for  $\gamma$ - and/or X-ray counting

Laboratory	Substrate	Number of dilutions	Dilution factors	Wetting or seeding agent	Ring diameter outer, inner (mm)	Diameter of active area (mm)	Range of source mass (mg)	Remarks
AECL	polyester tape	-	-	-	38, 25	< 6	16 to 58	1)
CBNM	VYNS	2	202.001 39.346 04	Ludox 1:10 <sup>4</sup>	74, 66	5	15 to 25	-
IER	aluminized mylar	4	39.27 375.4 36.823 347.43	-	27.5, 16	4 ± 1	9.3 to 43.3	-
IFIN	polyethylene 0.2 mm	1	10.540	-	30, 24	3	15 to 60	
IMM	polymer film	-	-	-	25, 18	4	100 to 150	
KSRI	collodion		2)	-	53, 38	3	17 to 18	
IMRI	mylar (40 $\mu$ m)	1	301.556 ± 0.015	-	3)	< 5	33 to 86	
NBS	mylar <sup>109</sup> Cd	-	121.959 8	Ludox 1:20 000	54, 38	6	12.820 to 60.206	4)
	mylar <sup>109</sup> Pd	1	6.606 391	Ludox 1:20 000	54, 38	6	11.436 to 35.383	
NPL	5)							
OMH	polystyrene	-		-	32	5	32 to 67	
PTB	CdCl <sub>2</sub>		1	-	30, 25	3	8 to 26	
UVVVR	polyethylene foil (25 mg cm <sup>-2</sup> )	2	29.927 7 27.682 8	-	44 6)	5	20 to 40	7)

- 1) active deposit sealed between two pieces of tape of 6.3 mg cm<sup>-2</sup> thickness
- 2) an undiluted solution was used for  $\gamma$ -ray measurement
- 3) no ring, two sandwiched mylar films of diameter 10 mm
- 4) the foils were cut out, rolled up and placed in the well
- 5) NPL measured the activity of the solution in standard 5 ml NBS ampoule
- 6) foil diameter
- 7) sources used for electron rate measurement were replaced on to polyethylene foil and covered by another foil

Table 6 - Liquid-scintillation counting

Laboratory	Counting vessel	Nb. of dilut.	Dilution factors	Diluent		Number of sources used	Range of source mass (mg)	Composition of the scintillation solution	Remarks	
				$\mu\text{g g}^{-1}$ of sol.	mol HCl per $\text{dm}^3$ of sol.					
IEA	polyethylene 20 ml	1	10.985 071	100	1	0.1	12	15 to 55	10 ml of "Atomlight" scintillation solution (NEN) with 0.6 ml of carrier solution (100 $\mu\text{g}$ of Cd in 0.1 M HCl)	TDCR method extended dead time: 4 $\mu\text{s}$
	glass 20 ml	2	1	10.985 071	100	1	0.1	11 12		
IER	glass 20 ml	3	4	39.27 375.4 36.823 347.43	20	0.1	16	9.7 to 60.7	10 ml of Aqualuma plus (Lumac)	live-time measurements
NAC	glass 20 ml	1	7.5	500	1		10	28.66 to 33.82	12 ml of a commercial xylene-based scintillation cocktail (INSTAGEL from Packard)	dead time: 1.1 $\mu\text{s}$ for conversion-electron counting
NBS	glass 3 ml	1	121.959 8	25		0.1	3	9.552 to 30.528	Beckman Readysolv HPb deaerated with argon gas; 30 $\mu\text{l}$ diethylhexyl phosphoric acid were used to chelate the radiocadmium; 10 ml of hexane or additional scintillator were added to the outer vial to provide an effective light guide (hexane) with increased $\gamma$ -ray cross section	$^{109}\text{Cd}$ sources used for the direct activity method and for the $^{109}\text{Pd}$ dead time: 1 $\mu\text{s}$
	10 ml						8	20.016 to 34.250		
15 ml	1						20.359			
20 ml	1						18.635			
	glass	2	6.606 391 21.032 26			0.1	3	11.213 to 22.698 0.537 4 to 2.116 03	10 ml Readysolv HPb scintillator with 50 $\mu\text{l}$ diethylhexyl phosphoric acid deaerated with argon gas prior to sample addition	$^{109}\text{Pd}$ used in the $^{109}\text{Pd}$ - $^{109}\text{Cd}$ comparison dead time: 1 $\mu\text{s}$
NIM		5							5 g PBD diluted in a toluene-alcohol solution (1:3.3) with 10 $\mu\text{g}$ $\text{CdCl}_2$ in 0.1 mol HCl per ml of scintillator	

1  $\mu\text{g ml}^{-1}$ ,  
4  $\text{H}_2\text{O}$  was added,

2 TDCR = triple-to-double coincidence ratio [4],  
5 hemispherical vessel with 15 mm radius

3 standard glass with reflecting caps,

Table 7 -  $4\pi$  proportional counters used by the participants

Laboratory	Wall material	Height of each half (mm)	Anode			Distance from source (mm)	Voltage applied (kV)	Gas	Pressure (MPa)	Discrimination level (keV)	Dead time ( $\mu$ s)
			Material	Diameter (mm)	Length (mm)						
AECL*	stainless steel	21	stainless steel	0.013	36	10	2.0 to 2.6	CH <sub>4</sub>	0.1	various	2.01
BIPM	Al	20	stainless steel	0.1	40	10	6.68	Ar + CH <sub>4</sub> (9:1)	1.1	36.2	2.5 15 <sup>2</sup>
CBM	Al	40	stainless steel	0.021	150	20	2.0 to 2.6	Ar + CH <sub>4</sub> (9:1)	0.3 to 0.5	0.5 to 100 <sup>3</sup>	9.7
ETL	brass	25	stainless steel	0.05	80	10	3.4	CH <sub>4</sub>	0.1	0.2	4.35
IFIN	silvered brass	24	gold-coated W	0.02	42	11	3.0	CH <sub>4</sub>	0.1	1	10
IMM	stainless steel	67	gold-coated Mo	0.03	130	27	3.4	Ar + CH <sub>4</sub> (9:1)	0.7	0.1	5
IPEN	brass	22.5	stainless steel # 302SS	0.025	40	13	3.3	Ar + CH <sub>4</sub>	1.0	30.7	3.22
KSRI	Al	28.3	stainless steel	0.051	53	14	6.0	Ar+CH <sub>4</sub> (9:1) <sup>6</sup>	1.31	31	3.03
LMRI	gold-coated lucite	27	stainless steel	0.02	160	12	2.9	Ar + CH <sub>4</sub>	1.0	~ 40	28
NIM	Cr-coated brass	36	gold-coated W	0.025	70	18	3.25	Ar + CH <sub>4</sub> (9:1)	0.68	33 to 35	4.0 $\pm$ 0.2
NPL	steel	120	gold-coated W	0.05	250	70	4.0	Ar + CH <sub>4</sub>	0.5	~ 1.0	15

Table 7 (cont'd)

Laboratory	Wall material	Height of each half (mm)	Anode				Voltage applied (kV)	Gas	Pressure (MPa)	Discrimination level (keV)	Dead time ( $\mu$ s)
			Material	Diameter (mm)	Length (mm)	Distance from source (mm)					
OMI	Al	20	stainless steel	0.021	40	10	3.65	Ar + CH <sub>4</sub>	1.1	37	2.999
PTB	Al	20	gold-coated Mo	0.1	40	10	7.3	Ar + CH <sub>4</sub> (9:1)	1.1	30	5
UVVVR	Fe	7	gold-coated W	0.05	135	20	3.79	Ar + CH <sub>4</sub> (9:1)	0.5	~ 33	6

\* Sample slide operated manually; some sources were counted over a range of voltages and others were counted with a fixed voltage

<sup>1</sup> Upper and lower walls which were facing the X-ray detector consisted of aluminized mylar foils of 0.9 mg cm<sup>-2</sup>

<sup>2</sup> Two dead times were applied:  $\tau_1$ , which is assumed to be extended and is calculated [8], comes from the apparatus, and  $\tau_2$ , of a non-cumulative type, is applied in order to correct for the losses

<sup>3</sup> Energy range of spectra taken. The live-time correction of the MCA was checked by concurrent integral counting at varying discriminator levels

<sup>4</sup> Gold-plated brass; ceiling material was aluminum 0.2 mm thick

<sup>5</sup> The top wall was made of 0.5 mm Al

<sup>6</sup> P-10 gas

<sup>7</sup> The counter was made of two semi-cylinders of length 140 mm and diameter 96 mm

Table 8 - Gamma- and X-ray detectors, dead times

Laboratory	Scintillation detectors						Phototube	Resolution (FWHM*)		Solid angle (sr/4π)	Semi-conductor detectors								
	Number of crystals		ordinary		well type			Resolution (%)	Resolution (keV)		Nature and type	Dimensions		Volume or relative efficiency (cm <sup>3</sup> )	Energy resol. FWHM* (keV) for ref. energy 88 keV	Window		Solid angle (sr/4π)	Dead times for γ- and/or X-ray channel (μs)
	ordinary	well type	diam. (mm)	height (mm)	diam. (mm)	depth (mm)						φ (mm)	h (mm)			material	thickness (mm)		
AECL	2 NaI(Tl)	-	50	1	-	-	34 (at 22 keV)	7.5	0.325	Coaxial Ge(Li)	48, 49	(88 ± 2)	1.3	Al	0.5	0.013 8	110		
CBM	2 CsI(Tl) <sup>1</sup>	-	51	25	-	-	20 (at 88 keV)	18	0.999								10.7		
ETL	NaI(Tl) <sup>2</sup>	-	3.75	2	-	-													
IBA	2 NaI(Tl) <sup>3</sup>		50	50															
IER	-	NaI(Tl)	127	127	28	75	13.8 (at 88 keV)	12.1	0.989								Live time		
IFIN										Ge(Li)	45, 60	100	2.5	Al	1	0.000 42	Live time		
IMM										Ge(Li)	50.25, 49	82	1.37	Al+Teflon	0.5 + 0.5	0.004 97	8		
KSRI										Ge high purity	10, 7	0.55	0.480	Be	0.13	20 <sup>4</sup>	3.06		
LMRI	-	NaI(Tl)	125	100	14.5	48.42	16.5 (at 88 keV)	14.5	1								4.2 (cumulative)		
NAC	CaF <sub>2</sub> (Eu) <sup>5</sup>	-	7.62	0.762	-	-											6.4, 1.1 <sup>7</sup>		
NBS	-	NaI(Tl)	50.8	50.8	8.2, <sub>6.7</sub> <sup>8</sup>	50.8	14.6 (at 88 keV)	12.9	0.987 0	Ge(Li)	-	70	0.99	Al	0.51	0.001	Live time		
OMH										Ge high purity	46, 35	55	0.95	Be	0.5	0.012 7 <sup>9</sup>	Live time		
PTB										Ge high purity	50, 62	127	1	Be	0.5	0.004 3			
UVVR	2 NaI(Tl)	-	44	20 <sup>10</sup>	-	-	15 (at 88 keV)	13.2	1								6		

\* full width at half maximum

<sup>1</sup> sandwich

<sup>2</sup> the detector was equipped with a Be window

<sup>3</sup> used for the X photon detection in the sum configuration

<sup>4</sup> distance between source and detector, in mm

<sup>5</sup> for the detection of 22 keV K X rays

<sup>6</sup> for the detection of conversion electrons

<sup>7</sup> for the conversion-electron channel

<sup>8</sup> hole in crystal; hole in detector

<sup>9</sup> distance from source to detector: 100 mm

<sup>10</sup> the NaI(Tl) crystals were covered with a 0.77 mg cm<sup>-2</sup> Al foil; a source inside polyethylene (PE) foils was placed between them.

Table 9 - Counting data for the different methods

Laboratory	Methods	Window limits or discrim. threshold (keV)	Typical count rates ( $s^{-1}$ )	Background rates ( $s^{-1}$ )	Number of sources measured	Typical time for one measurement (s)	Date of measurement
AECL	PC channel	0.1	2 600	0.5	6	400	86-03-14
	Ge(Li) for $^{109}\text{Pd}$	10	2 to 68	0.02	5	10 000	to
	Ge(Li) for $^{109}\text{Cd}$	10	2 to 68	0.02	6	10 000	86-04-24
BIPM	PPC channel	36.2	1 400 to 10 700	16	28	500 to 1 000	86-05-06 to 86-06-13
CBM	PPC channel	20	800 to 6 000	4 to 5	10	2 000	86-06
	CsI(Tl)	46	1 100 to 5 200	4.45	4	4 000 to 30 000	86-06
ETL	PC channel	0.2	8 000	5.1	22 (dil. 1) 17 (dil. 2)	500	86-05
IEA	TDCR channel <sup>1</sup>		71 000 to 87 000 13 000 to 41 000		not dil. 11 diluted 12	3 x 1 320 <sup>2</sup> 10 800	86-05-06 to 86-05-09
	LS channel	21 to 26	250 to 750 <sup>3</sup>			7 200 <sup>4</sup>	86-05-21
		62 to 86	5 500 to 16 000 <sup>5</sup> 70 to 210 <sup>6</sup>				
IER	LS channel	36.3 198	130 to 8 000	0.1	16	900 to 4 200	86-07-17 to 86-07-18
IFIN	PC channel	1	8 000	1.7	6	1 000	
	NaI(Tl) channel	10 to 30 (X rays)	400	0.7	6	1 000	86-07
	Ge(Li)	80 to 96	0.5 to 2	0.3	4	1 000	
IMM	PPC channel	36	700 to 2 000	7	10	1 000	86-05
	Ge(Li) channel	30	140 <sup>7</sup>	30	3	20 000	"
IPEN	PPC channel	30, 7	2 100	1.5	16	960	86-05-15 to 86-07-11
KSRI <sup>8</sup>	PPC channel	31, 0 integral	9 000	1.4	12	1 000	86-07 to
	Ge channel	65 to 100	9	0.68	4	3 000	86-08-02
LMRI	PPC channel	35	300	2	10	3 000	86-07
	NaI(Tl) channel	42.2 to 120	20 to 52	3.0 ± 0.03	4	21 600	"
NAC	LS channel	57	20 000	1.0	10	1 000	86-03-13
	Phototube channel	50	21 000	0.8	10	1 000	to
	CaF <sub>2</sub> (Eu) channel <sup>9</sup>		370	0.2	10	1 000	86-05-05

Table 9 (cont'd)

Labo- ratory	Methods	Window limits or discrim.threshold (keV)	Typical count rates (s <sup>-1</sup> )	Background rates (s <sup>-1</sup> )	Number of sources measured	Typical time for one measurement (s)	Date of measurement
NBS	LS channel	25	1 000	0.2	9	1 000	86-03
	NaI(Tl) channel	39	100	1.4	12	2 x 6 000	
	LS chan.for <sup>109</sup> Pd	1.5	1 000	10	3	500	86-03-13
	NaI(Tl) channel	39.0	16.500 ± 0.094 <sup>10</sup>	1.4	3	10 <sup>9</sup> Pd	
	Ge(Li) channel		16.548 ± 0.046 <sup>10</sup>			3 000	
NIM	PPC channel	33 to 35	6 000	1 to 2	30	1 200	86-04-21 to 86-05-23
NPL	PPC channel	37	700	9	14	1 200	86-05-01
	High pr. ioniz. chamber channel		1.437 2 <sup>11</sup>		1	50 000	to 86-05-13
OMH	PPC channel	37 integral	12 500 1 030	0.2	21	3 x 200 3 x 500	86-03-06 to
	Ge channel	4.0 integral	400	3.8	2	40 000	86-03-07
PTB	PPC channel	30	10 500	0.1	7	4 000	86-05-12
	Ge channel		250 integral 4.5 peak		3	40 000	to 86-05-27
UVVVR	PPC channel	33 to 166	5 500	4.0	2 x 11	8 x 40	86-03-20
	NaI(Tl) channel	(X <sub>K</sub> ) 5.9 to 58 (γ) 58 to 160	5 600 (N <sub>X</sub> ) 200 (N <sub>γ</sub> )	5.5 to 8.0	2 x 11	6 x 100	to 86-06-02

1 triple-to-double coincidence ratio method [4]

2 for 15 different efficiencies

3 for X-ray counting

4 each source was counted at 7 different efficiency points

5 for conversion electron counting

6 for coincidence counting

7 at peak

8 data from Ge(Li) detector were excluded due to difficulty in determining efficiency below 100 keV by means of <sup>133</sup>Ba

9 discrimination window set on the 22 keV peak

10 ratio <sup>109</sup>Cd/<sup>109</sup>Pd gamma-ray emission rate

11 current in pA/g

Table 10 - Formulae used for calculating the results

AECL - Method 1 [7] - Standardization of  $^{109}\text{Pd}$

$$N_0(^{109}\text{Pd}) = \frac{N(^{109}\text{Pd}+^{109}\text{Ag}^m)}{EF},$$

where

$N$  is the count rate taken at count midpoint and corrected for dead-time background, accidental coincidences, delay mismatch and decay,

$EF = 4\pi(\text{PC})$  efficiency for counting  $^{109}\text{Pd}+^{109}\text{Ag}^m = 1.9635 - 0.016$ , where the second term is the estimated self-absorption correction for the  $4\pi\beta$  counting of  $^{109}\text{Pd}$ . It leads to  $EF = 1.948 \pm 0.011$ .

$$T_{1/2}(^{109}\text{Pd}) = (13.402 \pm 0.006) \text{ h, and}$$

$$N_0(^{109}\text{Cd}) = \frac{N_0(^{109}\text{Pd}) \cdot 88 \text{ keV rate(Cd sources)}}{88 \text{ keV rate(Pd sources)}}.$$

- Method 2 [6] -  $4\pi\epsilon$ -X coincidence method for  $^{109}\text{Cd}+^{109}\text{Ag}^m$

$$N_{4\pi} = N_0 \left[ P_K(1 - \omega_K) \epsilon_{KA} + (P_K \omega_K + P_{LM}) \epsilon_{LM} + \frac{\alpha \epsilon_e + \epsilon_{\beta\gamma}}{1 + \alpha_t} \right],$$

$$N_X = N_0 \left[ P_K + \frac{\alpha_K}{1 + \alpha_t} \right] \omega_K \epsilon_X,$$

$$N_C = N_0 \left[ P_K \epsilon_{LM} + \frac{\alpha_K \epsilon_e}{1 + \alpha_t} \right] \omega_K \epsilon_X,$$

from which

$$N_0 = \frac{N_{4\pi} N_X}{N_C} \left[ 1 + \frac{\alpha_t + \epsilon_{\beta\gamma}}{1 + \alpha_t} \right]^{-1}, \quad \text{as } \epsilon_e \text{ and } \epsilon_{LM} \rightarrow 1$$

where

$\epsilon_{KA}$  is the probability of detecting an event in the  $4\pi\text{PC}$  resulting from a K-Auger transition,

$\epsilon_{LM}$  is the probability of detecting an event in the  $4\pi\text{PC}$  resulting from the filling of L, M, ..., shell vacancies,

$\epsilon_e$  is the probability of detecting an event in the  $4\pi\text{PC}$  resulting from the internal conversion of a 88 keV  $\gamma$  transition.

The other variables have the usual meanings.

An extrapolation to  $N_C/N_X = 1$  gives the value

$$N_{4\pi} = \left( 1 + \frac{\alpha_t + \epsilon_{\beta\gamma}}{1 + \alpha_t} \right) N_0 = (1.9635 \pm 0.0007) N_0$$

and therefore  $N_0$ .

Table 10 (cont'd)

BIPM

$$N_o = N_{ce} C_{exp} \frac{1 + \alpha_t}{\alpha_t + \epsilon_{\beta\gamma}},$$

where  $N_{ce}$  is corrected for background and decay (two dead times were applied), for the conversion electrons under the threshold and for the photons above the threshold.

CBNM

$$N_o = N_{ce+\gamma} (1 + C_{tail}) \quad (4\pi CsI),$$

$$N_o = N_{ce} \frac{1}{\epsilon_{ce}} \frac{1 + \alpha_t}{\alpha_t} \quad (4\pi PPC),$$

where

$N_{ce+\gamma}$  and  $N_{ce}$  are corrected for background and decay (live-time measurements were applied in all cases),

$C_{ce}$  and  $C_{\gamma}$  are correction terms for the conversion-electron and  $\gamma$ -emission rates,

$C_{tail}$  is a correction term to take into account the tail of the K electron distribution,

$\epsilon_{ce}$  is the  $4\pi(PPC)$  efficiency for the conversion electrons.

ETL [5] -  $4\pi e$ -X coincidence method

$$N_{ce} = N_o \left[ \frac{\alpha_t}{1 + \alpha_t} ((\epsilon_{ce})_T + (1 - (\epsilon_{ce})_T) \epsilon_{\beta X}) + R \omega_K \epsilon_{\beta X} + (1 - \frac{\alpha_t}{\alpha_t + 1}) \epsilon_{\beta\gamma} \right],$$

$$N_X = N_o \omega_K \epsilon_X \left( R + \frac{\alpha_K}{1 + \alpha_t} \right),$$

$$N_c = N_o \omega_K \epsilon_X (\epsilon_{ce})_K \frac{\alpha_K}{1 + \alpha_t},$$

where

$$R = \frac{EC(K)}{EC(K) + EC(L) + EC(M)}.$$

$\epsilon_X$  is the efficiency of the X channel for the 22 keV X rays,

$\epsilon_{\beta X}$  and  $\epsilon_{\beta\gamma}$  are the counting efficiencies of the ce channel for the 22 keV X rays and for the 88 keV  $\gamma$  rays,

Table 10 (cont'd)

$(\epsilon_{ce})_K$  and  $(\epsilon_{ce})_T$  are the counting efficiencies of the  $\beta$  channel for K and all conversion electrons.

The value  $\left(\frac{R \alpha_K}{1 + \alpha_t} + 1\right)$  is obtained experimentally and considering

$(\epsilon_{ce})_K < (\epsilon_{ce})_T < 1$ , as  $(\epsilon_{ce})_K \rightarrow 1$ ,

$$N_o = N_{ce} \left[ \frac{\alpha_t}{1 + \alpha_t} + R \omega_K \epsilon_{\beta X} + \left(1 - \frac{\alpha_K}{1 + \alpha_t}\right) \epsilon_{\beta \gamma} \right]^{-1} .$$

IEA - Method 1, TDCR (see ref. [4])

- Method 2, LS counting

$$N_o = \frac{N_e N_X \alpha_K}{N_c (\alpha + \phi)} ,$$

where  $N_e$  is the LS channel count rate,  $N_X$  the X channel count rate,  $N_c$  the coincidence channel count rate, and  $\phi$  is the LS channel efficiency.

The activity concentration was found by changing the high voltage.

In this case  $\left(1 - \frac{N_c}{N_X}\right) \frac{N_X}{N_c} \rightarrow 0$  and  $N \rightarrow N_o$ .

IFIN -  $4\pi(PC)ce-NaI(Tl)\gamma$

$$N_{ce} = N_o \frac{\alpha_K \epsilon_K + (\alpha_t - \alpha_K) \epsilon_L}{1 + \alpha_t} ,$$

$$N_X = N_o \omega_K \left( P_K + \frac{\alpha_K}{1 + \alpha_t} \right) \epsilon_X ,$$

$$N_c = N_o \omega_K \frac{\alpha_K}{1 + \alpha_t} \epsilon_X \epsilon_K ,$$

$$\frac{N_e N_X}{N_c} = N_o \left( P_K + \frac{\alpha_K}{1 + \alpha_t} \right) \left[ 1 + \frac{\epsilon_L}{\epsilon_K} \left( \frac{\alpha_t}{\alpha_K} - 1 \right) \right] ,$$

where

$\epsilon_K$  and  $\epsilon_L$  are efficiencies of the  $4\pi$  proportional counter for K and L,M conversion electrons,

$$\epsilon_L / \epsilon_K \approx 1.02 .$$

Table 10 (cont'd)

- Ge(Li) $\gamma$ 

$$N_o = \frac{N_\gamma}{\epsilon_\gamma P_\gamma} .$$

The experimental efficiency curve of the Ge(Li) detector was fitted by the function  $\ln(\epsilon_\gamma) = -1.836 (\ln E)^2 + 18.47 (\ln E) - 52.574$ , where E is the energy.

IPEN

$$N_o = N_{ce} C_{sp} \left( \frac{1 + \alpha_t}{\alpha_t + \epsilon_{\beta\gamma}} \right) ,$$

where

$C_{sp}$  is the spectrum extrapolation,

$N_{ce}$  is corrected for dead time, background, decay and extrapolated to energy 0.

KSRI

$$N_o = N_{ce} + N_\gamma ,$$

where  $N_{ce}$  and  $N_\gamma$  are corrected for dead time, decay and background.

LMRI

$$N_o = N_{ce} + N_\gamma ,$$

where

$N_{ce}$  is corrected for background and decay (cumulative dead times were applied) and extrapolated exponentially to 0 keV,

$N_\gamma$  is the result of  $4\pi\gamma$  counting.

NAC

$$N_o = \left( \frac{BG}{C} \right)^* \frac{k}{(\phi k + ec_K)} \quad (\text{LS counting method}),$$

where

B is the conversion-electron emission rate corrected for background, coincidence resolving times and satellite pulses,

G is the corrected K X-ray rate,

C is the corrected electron-X-ray coincidence rate,

$\left( \frac{BG}{C} \right)^*$  is the extrapolated value,

$\phi$  is the intensity of internal-conversion electrons,

k is the fraction of internal-conversion events in the K shell, and

$ec_K$  is the fraction of electron-capture events in the K shell.

Table 10 (cont'd)

NBS - Method 1, LS counting

$$N_o = N_{ce} + N_\gamma ,$$

where

$N_{ce}$  is corrected for dead time, background and decay,

$N_\gamma$  is the result of  $4\pi\gamma$  counting.

- Method 2, Standardization of  $^{109}\text{Pd}$

$$N_o(^{109}\text{Pd}) = \frac{N(^{109}\text{Pd} + ^{109}\text{Ag}^m)}{\text{EFT}} ,$$

where

$N$  is corrected for dead time, background, impurities ( $^{111}\text{Ag}$ ,  $^{24}\text{Na}$ ,  $^{56}\text{Mn}$ ),  
EFT (mean efficiency between the tracing method and the extrapolation method)  
= 1.9617, and

$$N_o(^{109}\text{Cd}) = \frac{N_o(^{109}\text{Pd}) \cdot 88 \text{ keV rate (Cd sources)}}{88 \text{ keV rate (Pd sources)}} .$$

NIM

$$N_o = N_{ce} C_{ce} C_{sp} \text{ (LS and PPC methods) ,}$$

where

$N_{ce}$  is corrected for background, dead time and decay,

$C_{sp}$  is the spectrum correction above threshold X rays and Auger electrons,

$$C_{ce} = \frac{1 + \alpha_t}{\alpha_t + \epsilon_{\beta\gamma}} .$$

NPL

$$N_o = N_{ce} + N_\gamma ,$$

where  $N_{ce}$  is corrected for dead time, background and decay.

OMH

$$N_o = N_{ce} C_{sp} C_s C_g + N_\gamma ,$$

where

$N_{ce}$  is corrected for dead time, background and decay,

$C_{sp}$  is the spectrum extrapolation,

$C_s$  is the self-absorption,

$C_g$  is the geometry loss.

PTB

$$N_o = N_{ce} + N_\gamma ,$$

where

$N_{ce}$  is corrected for dead time, background and decay,

$N_\gamma$  is the result of the measurement of  $\gamma$  rate.

UUVVR

$$N_o = \frac{N_{ce} K_D}{I_{ce}} ,$$

$$N_o = \frac{N_X K_D K_{DL}}{I_{XK} \epsilon_X} ,$$

$$N_o = \frac{N_\gamma K_E}{I_\gamma \epsilon_\gamma} ,$$

where

$N_{ce}$  is the conversion electron count rate,

$N_X$  is the X-photon count rate,

$N_\gamma$  is the  $\gamma$ -ray count rate,

$K_D$  is the correction for discrimination,

$K_{DL}$  is the correction for dead layer,

$K_E$  is the correction for secondary-electron escape,

$\epsilon_X$  is the detection efficiency of X rays,

$\epsilon_\gamma$  is the detection efficiency of  $\gamma$  rays,

$I_{ce}$ ,  $I_{XK}$  and  $I_\gamma$  are the emission probabilities of the conversion electrons, the K X rays and the  $\gamma$  rays, respectively.

Table 11 - Corrections applied for calculating the results

Laboratory and method	$C_{sp}^*$	Pile-up	Background	Radioactive decay	$\alpha_t$	Remarks
AECL					$26.8 \pm 0.3$	Ge(Li): loss correction for random summing and pile-up.
BIEM PFC	0.017%				$26.4 \pm 0.5$ [10]	Result derived only from conversion-electron counting.
CBNM PFC	0.07 to 0.54	$10^{-4}$ to $1.5 \cdot 10^{-3}$	$6.6 \cdot 10^{-4}$ to $7.8 \cdot 10^{-3}$	1.07 to 1.08		Spectrum extrapolation for conversion electrons below the threshold of the form $N_{ce} = \exp(a + b C)$ .
$4\pi$ -CsI(Tl) sandwich spectrometer	0.3% to 0.7%	0.15% to 0.75%	0.002% to 0.7%	0.12% to 0.14%		$1 - P_\gamma = 0.9639 \pm 0.0004$ was used. a)
ETL					26.173 9	
IEA TDCR						Escape probabilities of X and $\gamma$ calculated by using the simulation method [16]. Effects of ionization quenching calculated according to Birks's formula [16], $k_B = 0.162$ .
$4\pi$ (LS)e-X					26.45 ( $\alpha_K = 11.3$ )	$\phi = 0.162$ to $0.174$ .
IER (LS)ce	1.5%					Mass-dependent loss of efficiency: 0.2% to 0.6%.
(LS) $\gamma$	1.3%	0.8% to 2.4% b)				Absorption in the well liner: 0.84%.
IFIN $4\pi$ (PPC)-NaI					$26.4 \pm 0.3$ ( $\alpha_K = 11.3$ )	$\epsilon_K/\epsilon_L \approx 1.02$ . $N_e$ is corrected for X, $\gamma$ sensitivity.

Table 11 (cont'd)

Laboratory	$C_{sp}^*$	Pile-up	Background	Radioactive decay	$\alpha_t$	Remarks
IMM					$26.4 \pm 0.4$	Result is only derived from conversion-electron rate. Extrapolation below the threshold for conversion electrons.
IPEN	$1.0016 \pm 0.0016$				$26.4 \pm 0.5$	$\epsilon_{\beta\gamma} = (0.3 \pm 0.3)\%$ . Extrapolation to 0 keV for conversion-electron spectrum.
LMRI	0.18%	-0.34% to -( $0.85 \pm 0.05$ )% c)				Extrapolation from 0 to 35 keV ( $A e^{-\beta C} \approx 0.18\%$ ; $\gamma$ counting under threshold: ( $0.12 \pm 0.1$ )%; Bremsstrahlung from conversion electrons above threshold: -( $0.61 \pm 0.2$ )%; detection efficiency: ( $0.7 \pm 0.02$ )%.
NAC					26.4	Coincidence resolving time: 0.57 $\mu$ s. Satellite pulses: 0.14% to 0.36%.
$4\pi e-4\pi e$ coincidence						
$4\pi(1S)e-X$ coincidence						Coincidence resolving time: 0.57 $\mu$ s. Satellite pulses: 0.30% to 0.39%. $\phi = 0.9635$ ; $k = 0.4276$ ; $e_{KX} = 0.788$ [10]. The X-ray counts were reduced by 0.24% to account for 88 keV $\gamma$ -Compton events falling within the window set on the 22 keV peak.
NBS (1S)ce	0.11% d)					Correction for the accidental coincidences according to a linear and weighted least-square fit on the count rates versus the masses of the $^{109}\text{Cd}$ solution. Detection of conversion electrons above 39 keV:-( $0.41 \pm 0.13$ )%. Photoelectric absorption in the liner: ( $0.45 \pm 0.07$ )%. Count rate below 39 keV. Photoelectron escape: ( $0.09 \pm 0.03$ )%. Compton backscatter: ( $0.01 \pm 0.01$ )%. Bremsstrahlung in NaI: ( $0.02 \pm 0.02$ )%. Photoelectric absorption in the mylar foil: 0.007%. Backscatter from the shield, phototube and liner:-( $0.2 \pm 0.1$ )%.

Table 11 (cont'd)

Laboratory	$C_{sp}^*$	Pile-up	Background	Radioactive decay	$\alpha_t$	Remarks
NBS (cont'd) $^{109}\text{Pd}$ standardization						A 60 Hz pulser peak was used to correct for losses due to pulse pile-up: $C_{\max}$ 6% ( $^{109}\text{Pd}$ ) at a total rate above amplifier noise of $1\,700\text{ s}^{-1}$ . For $^{109}\text{Cd}$ , $C_{\max} = 2\%$ .
NIM	$1.000 \pm 0.002$				$26.4 \pm 0.5$	$\epsilon_{\beta\gamma} = 0.001\,7$
NPL	0.05%					Self-absorption: 0.15%; K-X rays above threshold: -0.01%; detection of 88 keV $\gamma$ rays in PPC: -0.03%.
QMH	$1.002 \pm 0.002$					Geometry loss: $C_g = 1.001\,6 \pm 0.000\,5$ ; Source self-absorption = $1.000\,3 \pm 0.000\,3$ .
PTB	e)					
UVVVR K X measurement	f)				$26.4 \pm 0.3$	$K_D = 1.008\,7 \pm 0.000\,4$ $K_{DL} = 1.005\,5 \pm 0.001\,2$ $\epsilon_X = 0.977 \pm 0.007\,3$
$\gamma$ measurement						$K_E = 1.007 \pm 0.001\,5$ $\epsilon_\gamma = 0.989 \pm 0.004\,8$

\*  $C_{sp}$  = correction applied for spectrum extrapolation (conversion electrons below the threshold and X rays above it).

a) Solid angle: 0.04%; foil absorption: 0.1%; life-time MCA: 0.3% to 4.4%.

b) Pile-up contribution between 36 keV and 50 keV.

c) X-ray pile-up above 42.2 keV.

d) Solid angle:  $(1.30 \pm 0.05)\%$ .

e) The portion of the conversion electrons below 30 keV was estimated by extrapolating the shape of the K-conversion-electron spectrum to zero energy. This shape was taken from a spectrum gated with K X rays from the NaI detector housing the proportional counter.

f) Correction for loss of a low-energy tail of the K-X IM peak below the discrimination level. The correction was determined by measuring the dependency of the count rate on pressure. The count rate is saturated if the pressure is equal to 0.9 MPa. For 0.5 MPa the correction mentioned is  $(1.7 \pm 0.18)\%$ .

Table 12 - Uncertainty components of the final result (in %)

Components due to Method	AECL		BLM		CBNM	ETL
	$4\pi$ e standardiz. of $^{109}\text{Pd}$	$4\pi$ -Auger electr. -X-ray coincid.	$4\pi$ (PPC)	$4\pi$ (PPC)	$4\pi$ CsI(Tl) sandw.spectrom.	$4\pi$ e-X coincidence
Counting statistics	0.68	0.69	0.01	0.2	0.1	0.2
Weighing	< 0.02	0.02	0.07	0.1	0.1	0.3
Dead time	0.10	0.02		0.1	0.15	0.1
Resolving time						( $\delta t_d$ : $\pm 0.05 \mu\text{s}$ )
Delay mismatch						
Pile-up	included in dead time			0.1	0.2	0.02
Background	< 0.05	0.01	0.02	0.1	0.1	0.05
Timing	< 0.05	< 0.05				0.02
Adsorption	< 0.01	< 0.01				0.02
Impurities	long-lived $\beta$ impur. in $^{109}\text{Cd}$	< 0.01				0.05
Efficiency for PC counting of $^{109}\text{Pd} + ^{109}\text{Ag}^m$	0.01					measured with a Ge detector
Source self-absorption						
Uncertainty in $C_{ce}$						
Correction for below-threshold electrons and above-threshold X rays						
Foil absorption					0.1	
Threshold setting						
Correction for geometry loss						
Measurement of $\gamma$ rate						
- by Ge(Li)						
- by NaI						
Half life	0.05 for $^{109}\text{Pd}$					
Dilution			0.02	0.1	0.1	
Extrapolation for $4\pi\gamma$ counting						0.5
Efficiency for $4\pi\gamma$ counting	0.036					
$\alpha_t$	0.04	0.04		0.04		
$\epsilon_{\beta\gamma}$	0.03	< 0.01 [10]		0.1		
Accidental coincidences		< 0.02				
Tailing			0.24	0.1	0.15	
Solid angle					0.1	
Normalizing factor $(\alpha + \epsilon_{\beta\gamma})/(1+\alpha)$			0.05			
Decay data						
X and $\gamma$ escape probability						
Ionization quenching						
Mass-dependent loss of efficiency						
Combined uncertainty	0.70	0.69	0.26	0.34	0.38	0.63

Table 12 (cont'd)

Components due to Method	IEA		IER	IFIN	IMM	IPEN	KSRI	IMRI
	TDCR	$4\pi(\text{LS})e^-$ X coincid.	$4\pi(\text{LS})e$	$4\pi(\text{PC})-$ NaI(Tl) coincid. & Ge(Li) $\gamma$	$4\pi(\text{PEC})$	$4\pi(\text{PPC})$	$4\pi(\text{PPC})$	$4\pi(\text{PPC})$
Counting statistics	0.12 <sup>2</sup>	0.774 <sup>3</sup>	0.1 <sup>6</sup>	0.078	0.1	0.1	0.18 <sup>16</sup>	0.06
Weighing	0.14	0.142	0.042 <sup>7</sup>	0.039	0.1	0.05	0.03	0.02
Dead time		$\Delta\tau/tN_c =$ 0.010	0.01	0.008	0.001	0.02	0.02	
Resolving time								
Delay mismatch								
Pile-up		0.162 <sup>4</sup>			0.01			
Background	0.000 <sup>1</sup>	0.009	0.013 <sup>8</sup>	0.008	0.05	0.005	0.01	0.013
Timing	0.005	0.001	0.01		0.001	0.005	0.005	0.005
Adsorption	0.002 <sup>5</sup>	0.002		0.039		0.009		
Impurities				0.039				
Efficiency for PC counting of $^{109}\text{Pd} + ^{109}\text{Ag}^m$								
Source self-absorption								
Uncertainty in $C_{ce}$						0.067		
Correction for below-threshold electrons and above-threshold X rays			0.5 <sup>9</sup>			0.160	0.25	0.06
Foil absorption								
Threshold setting					0.1 <sup>15</sup>			
Correction for geometry loss				0.116 <sup>11</sup>				
Measurement of $\gamma$ rate								
- by Ge(Li)							0.06	
- by NaI								0.01
Half life	0.016	0.022			0.005		0.008	0.01
Dilution	0.02	0.02						0.005
Extrapolation for $4\pi\gamma$ counting								
Efficiency for $4\pi\gamma$ counting				0.233 <sup>12</sup>				
$\alpha_t$		0.163 <sup>5</sup> and $\alpha_x$		0.62 <sup>13</sup>	0.07			
$\epsilon_{\beta\gamma}$						0.01		
Accidental coincidences								
Tailing								
Solid angle								
Normalizing factor $(\alpha + \epsilon_{\beta\gamma})/(1+\alpha)$								
Decay data	0.55							
X and $\gamma$ escape probability	0.1							
Ionization quenching	0.5							
Mass-dependent loss of efficiency			0.1 <sup>10</sup>					
Combined uncertainty	0.77	0.83	0.52	1.51 <sup>14</sup>	0.2	0.21	0.32	0.26

Table 12 (cont'd)

Components due to Method	NAC		NBS		NIM		NPL
	$4\pi e-4\pi e$ coincid.	$4\pi(1S)e-X$	$4\pi(1S)$	$^{109}\text{Pd}$ standardiz.	$4\pi(\text{PPC})$	$4\pi(1S)$	$4\pi(\text{PPC})$
Counting statistics	0.05 <sup>17</sup>	0.17 <sup>20</sup>	0.12	0.30	0.11	0.05	0.02
Weighing	0.01	0.01	0.06	0.05	0.033	0.04	0.05
Dead time	0.015	0.023	0.05 <sup>24</sup>	0.05	0.1	0.02	0.02
Resolving time	0.001	0.012					
Delay mismatch							
Pile-up			0.12				0.05
Background	0.001	0.057 <sup>21</sup>				0.02	0.1
Timing			0.001 <sup>26</sup>				0.005
Adsorption			0.01	0.08	0.1		0.05
Impurities			0.01	0.16			0.05
Efficiency for PC counting of $^{109}\text{Pd}+^{109}\text{Ag}^m$							
Source self-absorption					0.033		0.15
Uncertainty in $C_{ce}$					0.024	0.07	
Correction for below-threshold electrons and above-threshold X rays					0.5	0.2	0.2
Foil absorption							0.05
Threshold setting							0.05
Correction for geometry loss							
Measurement of $\gamma$ rate							0.10 <sup>28</sup>
- by Ge(Li)							
- by NaI							
Half life	0.003 <sup>18</sup>	0.003 <sup>18</sup>			0.03		
Dilution						0.1	
Extrapolation for $4\pi\gamma$ counting				0.20			
Efficiency for $4\pi\gamma$ counting							
$\alpha_t$							0.01
$\epsilon_{\beta\gamma}$							
Accidental coincidences							
Tailing							
Solid angle							
Normalizing factor $(\alpha+\epsilon_{\beta\gamma})/(1+\alpha)$				0.04 (on $P_\gamma$ )			
Decay data		0.55 <sup>22</sup>					
X and $\gamma$ escape probability							
Ionization quenching							
Mass-dependent loss of efficiency							
Combined uncertainty	0.16 <sup>19</sup>	0.68 <sup>23</sup>	0.47 <sup>27</sup>	0.48	0.6	0.24	0.31 <sup>29</sup>

Table 12 (cont'd)

Components due to Method	OMH	PTB	UVVVR		
	4 $\pi$ (PPC)	4 $\pi$ (PPC)	4 $\pi$ (PPC)	K X-ray emission rate	$\gamma$ -ray emission rate
Counting statistics	0.09	0.05	0.08, 0.10 <sup>30</sup>	0.074, 0.08 <sup>30</sup>	0.07, 0.1 <sup>30</sup>
Weighing	0.01	0.02			
Dead time	0.005	0.02	0.001	0.001	< 0.001
Resolving time					
Delay mismatch					
Pile-up		0.01	0.015		
Background	0.01		0.004	0.003	0.03
Timing	0.005				
Adsorption	< 0.005		< 0.001	< 0.001	
Impurities	< 0.000 1		0.001	0.001	0.001
Efficiency for PC counting of $^{109}\text{Pd}+^{109}\text{Ag}^m$					
Source self-absorption	0.03				
Uncertainty in $C_{ce}$					
Correction for below-threshold electrons and above-threshold X rays	0.20				
Foil absorption					
Threshold setting	0.10				
Correction for geometry loss	0.05				
Measurement of $\gamma$ rate					
- by Ge(Li)	0.09	0.06			
- by NaI					
Half life	< 0.002				
Dilution					
Extrapolation for $4\pi\gamma$ counting					
Efficiency for $4\pi\gamma$ counting					
$\alpha_t$					
$\epsilon_{\beta\gamma}$					
Accidental coincidences					
Tailing		0.33 (ce)			
Solid angle					
Normalizing factor $(\alpha + \epsilon_{\beta\gamma})/(1+\alpha)$					
Decay data					
X and $\gamma$ escape probability					
Ionization quenching					
Mass-dependent loss of efficiency					
Combined uncertainty	0.27	0.34	0.21 <sup>31</sup>	1.1 <sup>32</sup>	1.1 <sup>33</sup>

Table 12 (cont'd)

Notes

- 1 Including uncertainties on dilutions.
- 2 99% confidence level, 22 degrees of freedom.
- 3 99% confidence level, 11 degrees of freedom.
- 4  $\frac{\Delta\tau}{\tau} (N_1 + N_2 - 2 \frac{N_1 N_2}{N_c})$ .
- 5  $\Delta\alpha_K/\alpha_K^2$ .
- 6 Standard deviation of the mean of the results of 4 different dilutions.
- 7 0.018% from dilution, 0.038% from source preparation.
- 8 Standard deviation of background/source count rate.
- 9 1/3 of maximum possible deviation.
- 10 Standard deviation of the slope of a linear extrapolation to zero mass.
- 11 Measured with a Ge(Li); uncertainty on efficiency curve: 0.39%, and  $P_\gamma = 0.43\%$ .
- 12 Efficiency ratio.
- 13 Uncertainty on  $P_K$ ,  $\alpha_K$  and  $\alpha_L$ .
- 14 1.09% for the Ge(Li) measurement.
- 15 Including uncertainty on spectrum extrapolation.
- 16 Standard error for 11 sources.
- 17 Standard deviation of 15 measurements.
- 18 Uncertainty on the decay correction.
- 19 Other contributions are due to the fitting of data: 0.15%, and to the presence of satellites: 0.025%.
- 20 Standard deviation of 10 measurements.
- 21 Entirely due to X-ray background uncertainty.
- 22 Decay-scheme parameters; uncertainties on  $\phi = 0.07\%$ , on  $k = 1.87\%$ , and on  $ec_k = 1.27\%$ .
- 23 Other contributions come from the fitting of the data: 0.35%, and from the presence of satellites: 0.047%.
- 24 Live time.
- 25 Included in counting statistics.
- 26 Timing and decay.
- 27 Other contributions are due to the total correction factor: 0.41%, the source position: 0.04%, the detector dimensions: 0.04%, the energy calibration: 0.07%, and the extrapolation to 39.0 keV: 0.04%.
- 28 Measurements performed with a high-pressure ionization chamber, type PA782.
- 29 Uncertainty on  $N_\gamma$  mainly due to interpolation of calibration curve of ionization-chamber response with energy and to assumed  $N_0$  and  $P_\gamma$  values of calibration points (random: 0.4%, interpolation: 2.2%,  $N_0$ : 1.7%,  $P_\gamma$ : 0.4%, others:  $\approx 0.6\%$ ).
- 30 For the first and second sets of sources.
- 31 Other contributions:  $\Delta K_D/K_D = 0.18\%$ ,  $\Delta I_E/I_E = 0.05\%$ .
- 32 Other contributions:  $\Delta I_{XK}/I_{XK} = 0.8\%$ ,  $\Delta\epsilon_X + \Delta K_{DL} = 0.74\%$ .
- 33 Other contributions:  $\Delta I_\gamma/I_\gamma = 1\%$ ,  $\Delta\epsilon_\gamma + \Delta K_\epsilon = 0.5\%$ .

Table 13 - Main uncertainty components of the final result

Laboratory	Main contributions to the combined uncertainty	Value of the main contributions (%)	Total uncertainty (%)	Method
AECL	counting statistics	0.68	0.70	<sup>109</sup> Pd standardization + Ge(Li) comp. 4 $\pi$ Auger electrons, X-ray coincidence
	counting statistics	0.18	0.20	
BIM	extrapolation below threshold	0.24	0.26	4 $\pi$ (PPC)ce
CBM	counting statistics	0.2	0.34	4 $\pi$ (PPC)ce
	dead time, tail extrapolation, pile-up	0.15, 0.15, 0.2	0.38	4 $\pi$ CsI(Tl)
EIL	efficiency extrapolation weighing, counting statistics	0.5 0.3, 0.2	0.63	4 $\pi$ e-X coincidence
IEA	decay data	0.21	0.30	TDCR
	ionizing quenching	0.19		
	counting statistics	0.30	0.32	4 $\pi$ (LS)e-X coincidence
IER	correction for spectrum extrapolation	0.5	0.52	4 $\pi$ (LS)ce+4 $\pi$ NaI(Tl) $\gamma$
IFIN	$P_K, \alpha_K, \alpha_L$	0.62	1.67	4 $\pi$ (PC)-NaI coincidence Ge(Li)
	efficiency curve	0.39	1.51	
	$P_\gamma$	0.43		
IMM	counting statistics	0.1	0.2	4 $\pi$ (PPC)ce
	threshold, extrapolation	0.1		
	weighing	0.1		
IPEN	counting statistics	0.1	0.21	4 $\pi$ (PPC)ce
	spectrum extrapolation	0.16		
KSRI	counting statistics	0.18	0.32	4 $\pi$ (PPC)ce-Ge $\gamma$
	spectrum extrapolation below and above threshold	0.25		
LMRI	counting statistics	0.06	0.09	4 $\pi$ (PPC)ce+4 $\pi$ NaI(Tl) $\gamma$
	extrapolation from 0 keV to 35 keV	0.06		
NAC	fitting of data	0.15	0.16	4 $\pi$ e-4 $\pi$ e(LS) coincidence counting 4 $\pi$ (LS)e-X
	counting statistics	0.17		
	fitting of data	0.35	0.68	
	decay scheme parameters	0.55		
NBS	total correction factor	0.41	0.47	4 $\pi$ (LS)ce+4 $\pi$ NaI(Tl) $\gamma$ <sup>109</sup> Pd standardization NaI(Tl)
	counting statistics	0.30		
	extrapolation to zero energy	0.20	0.48	
	impurities	0.16		

Table 13 (cont'd)

Laboratory	Main contributions to the combined uncertainty	Value of the main contributions (%)	Total uncertainty (%)	Method
NIM	spectrum extrapolation	0.5	0.6	$4\pi(\text{PPC})\text{ce}$
	spectrum extrapolation	0.2	0.24	$4\pi(\text{LS})\text{ce}$
	dilution	0.1		
NPL	spectrum extrapolation below and above threshold	0.2	0.31	$4\pi(\text{PPC})\text{ce}$
	source self-absorption	0.15		
	background	0.1		
OMH	spectrum extrapolation below and above threshold	0.2	0.27	$4\pi(\text{PPC})\text{ce-Ge}\gamma$
PTB	spectrum extrapolation	0.33	0.34	$4\pi(\text{PPC})\text{ce-Ge}\gamma$
UVVVR	counting uncertainties	0.08 to 0.10	0.21	$4\pi(\text{PC})\text{ce}$
	correction for discrimination	0.18		
	emission intensity of KX	0.8	1.1	K X-ray emission rate $4\pi\text{NaI(Tl)}$
	correction for dead layer, detection efficiency	0.74		
	emission intensity of $\gamma$	1.00	1.1	$4\pi\text{NaI(Tl)}\gamma$
	detection efficiency, correction for secondary electron escape	0.5		

Table 14 - Final results

Laboratory	Activity concentration (kBq g <sup>-1</sup> ) at reference date (1986-03-01, 00 h UT)	Combined uncertainty (kBq g <sup>-1</sup> )	Photon emission rate (s <sup>-1</sup> g <sup>-1</sup> )	Combined uncertainty (s <sup>-1</sup> g <sup>-1</sup> )	Remarks
AECL 109Pd stand. 4πe-X coincidence	6 026 5 990	42 12	219.9•10 <sup>3</sup>	4.2•10 <sup>3</sup>	
BIRM 4π(PPC)ce	5 976	16			
CBNM 4π(PPC)ce 4πCsI(TL) sandwich spectr.	5 967 5 980	20 24			
EIL 4πe-X coincidence	6 001	38			
IEA TDCR	6 019	46			(6 016 ± 49) kBq g <sup>-1</sup> for the non-diluted solution (6 022 ± 46) kBq g <sup>-1</sup> for the diluted solution
4π(LS)e-X	6 009	49			
IER 4π(LS)ce + 4πNaI(TL)γ	5 954	31	217.4•10 <sup>3</sup>	1.5•10 <sup>3</sup>	
IFIN 4π(PC)ce-NaI(TL)X Ge(Li)	6 480 6 400	110 100	234•10 <sup>3</sup>	6•10 <sup>3</sup>	(6 440 ± 70) kBq g <sup>-1</sup>
IMM 4π(PPC)ce	5 968	12	214•10 <sup>3</sup>	7•10 <sup>3</sup>	
IPEN 4π(PPC)ce	6 000	13			
KSRI 4π(PPC)ce	5 994	19	221.85•10 <sup>3</sup>	3.6•10 <sup>3</sup>	
IMRI 4π(PPC)ce	5 967	5.4	214.6•10 <sup>3</sup>	0.6•10 <sup>3</sup>	

Table 14 (cont'd)

Laboratory	Activity concentration (kBq g <sup>-1</sup> ) at reference date (1986-03-01, 00 h UT)	Combined uncertainty (kBq g <sup>-1</sup> )	Photon emission rate (s <sup>-1</sup> g <sup>-1</sup> )	Combined uncertainty (s <sup>-1</sup> g <sup>-1</sup> )	Remarks
NAC					
4πe-4πe-LS coincid.	6 033	9.7			
4π(LS)e-X	6 026	41			
NBS					
4π(LS)ce+4πNaI(Tl)γ	5 940	28	219.1·10 <sup>3</sup>	1.0·10 <sup>3</sup>	
<sup>109</sup> Pd stand.	6 006	29			
NIM					
4π(PFC)ce	6 027	34			
(LS) counting	6 030	15			
NPL					
4π(PFC)ce	5 979	19	213.5·10 <sup>3</sup>	6.2·10 <sup>3</sup>	
OMH					
4π(PFC)ce	5 978	16	218.1·10 <sup>3</sup>	5.1·10 <sup>3</sup>	
PTB					
4π(PFC)ce+Geγ	5 983	20	220.2·10 <sup>3</sup>	2.4·10 <sup>3</sup>	
UVVVR					
4π(PFC)ce	6 098	13			
K X-ray emission rate } 4πNaI(Tl)					
4πNaI(Tl)γ	6 000	67	219·10 <sup>3</sup>	1.1·10 <sup>3</sup>	

Tables 15, 16 and 17 (see pp. 12 and 13)

Table 18 - Values of the conversion electron and of the  $\gamma$ -ray emission rates obtained by performing the  $^{109}\text{Cd}$  activity measurements

Laboratory	Conversion-electron rate $10^6(\text{s}^{-1} \text{g}^{-1})$	Uncertainty $10^6(\text{s}^{-1} \text{g}^{-1})$	$\gamma$ -ray emission rate $10^6(\text{s}^{-1} \text{g}^{-1})$	Uncertainty $10^6(\text{s}^{-1} \text{g}^{-1})$
IER	5.737	0.030	0.217 4	0.001 5
IMM	5.750	0.010	0.214	0.007
KSRI	5.772 04	0.016 42	0.221 85	0.003 66
LMRI	5.752	0.004	0.214 6	0.000 6
NBS	5.721	0.028	0.219 1	0.001
NPL	5.765	0.017	0.213 5	0.006 2
OMH	5.759 9	0.014 3	0.218 1	0.005 1
PTB	5.762	0.020	0.220 2	0.002 4
UVVVR	5.875	0.012	0.219	0.001 1

Table 19 - Values of the  $\gamma$ -ray emission probabilities deduced from the conversion-electron and  $\gamma$ -ray emission rates listed in Table 18

Laboratory	$P_\gamma$	$\Delta P_\gamma$
IER	0.036 51	0.000 30
IMM	0.035 88	0.001 13
KSRI	0.037 01	0.000 60
LMRI	0.035 97	0.000 10
NBS	0.036 88	0.000 24
NPL	0.035 71	0.001 01
OMH	0.036 48	0.000 83
PTB	0.036 81	0.000 41
UVVVR	0.035 94	0.000 19

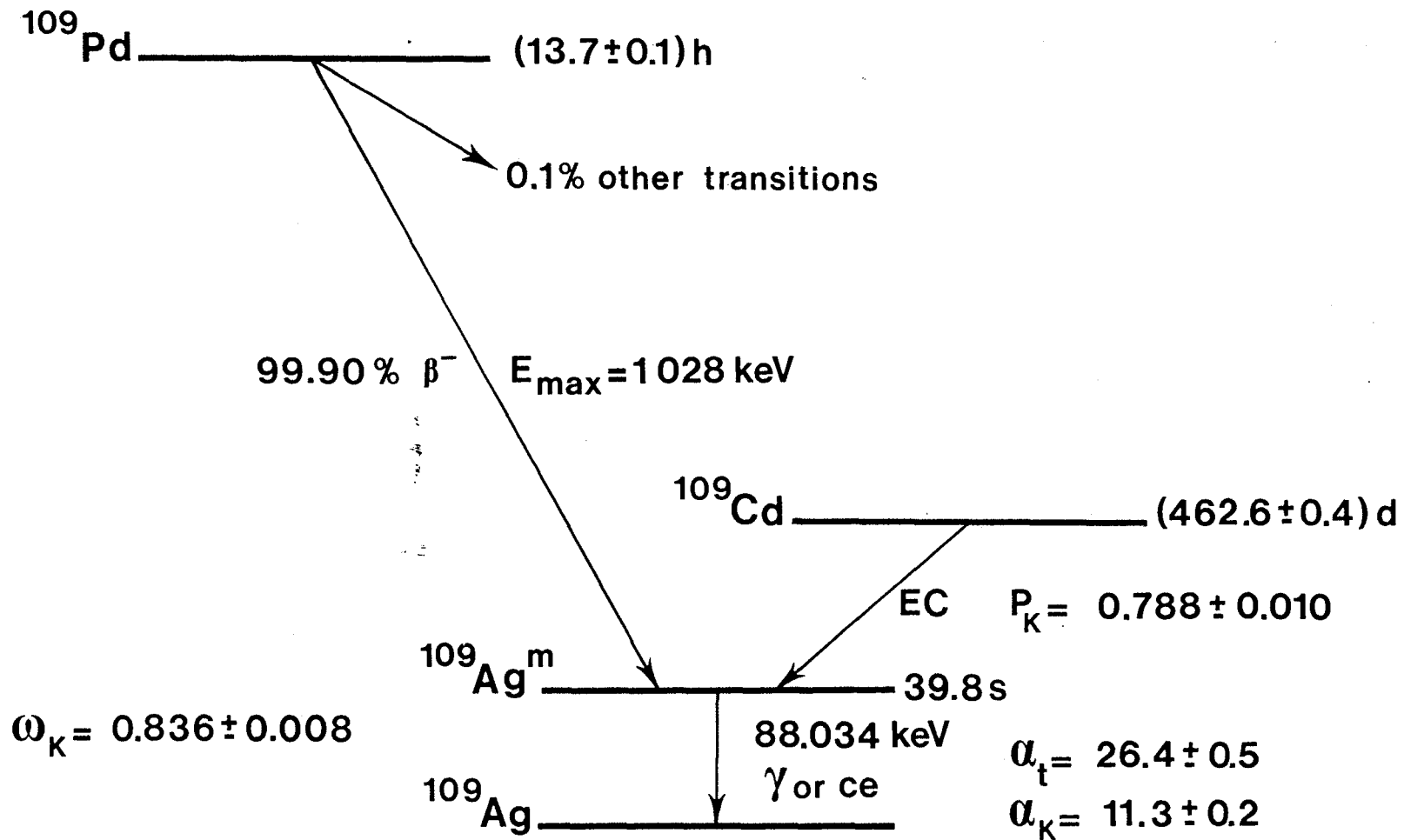


Fig. 1 - Decay scheme of  $^{109}\text{Cd}$  and  $^{109}\text{Pd}$  adapted from [14].

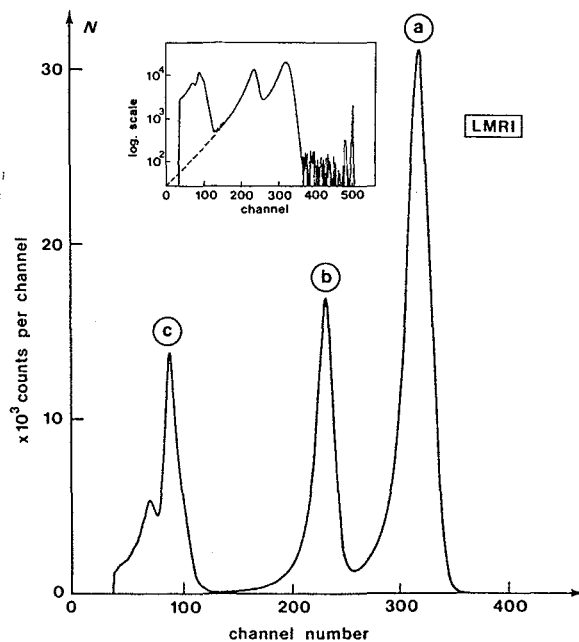
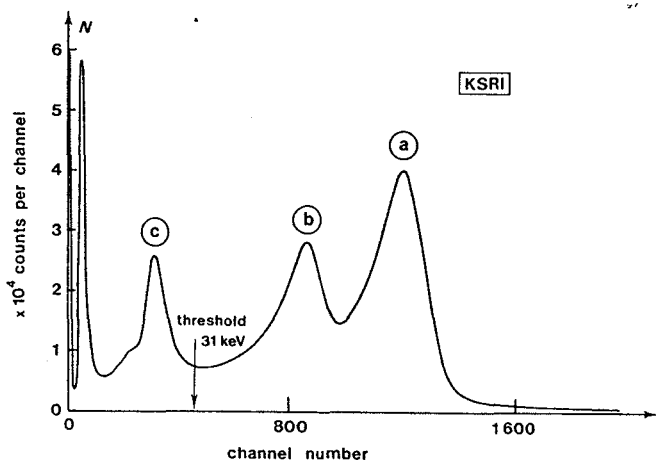
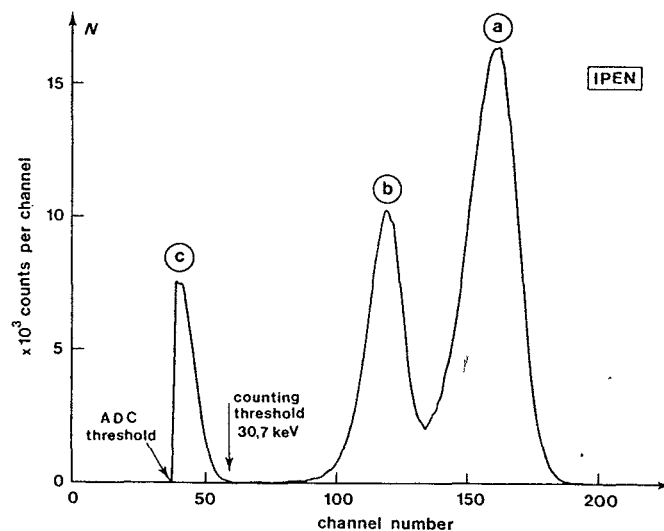
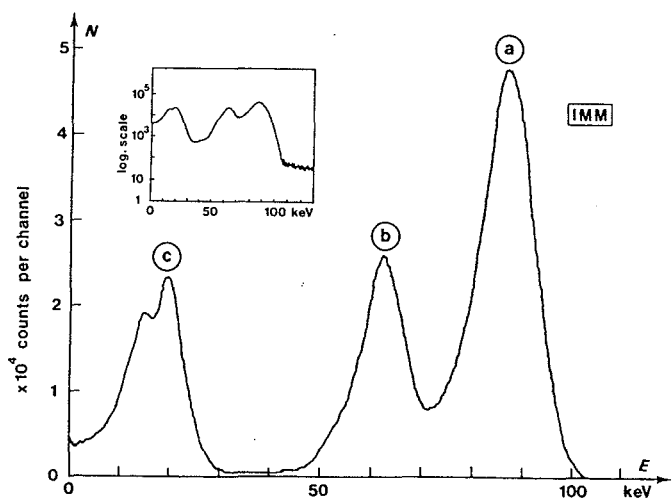
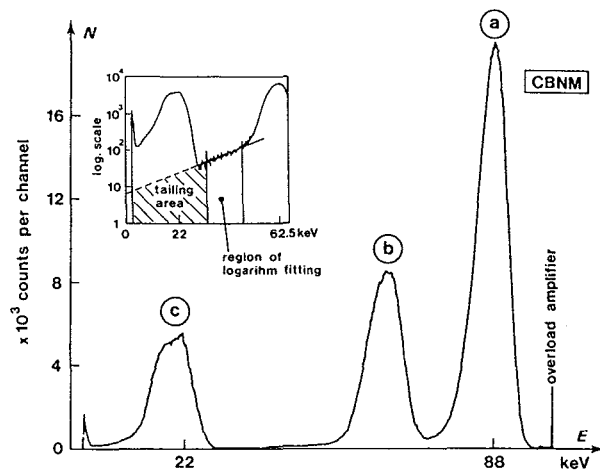
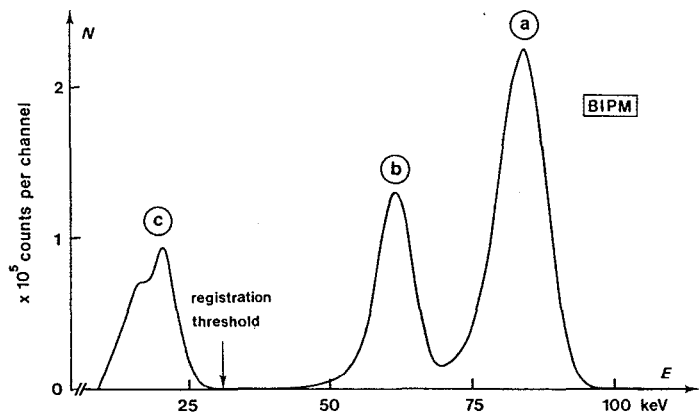


Fig. 2.1 - Some typical spectra obtained by means of a pressurized proportional counter. The letters a, b and c refer to the L, M, N conversion-electron peak, the K conversion-electron peak and the Auger and X-ray peaks, respectively.

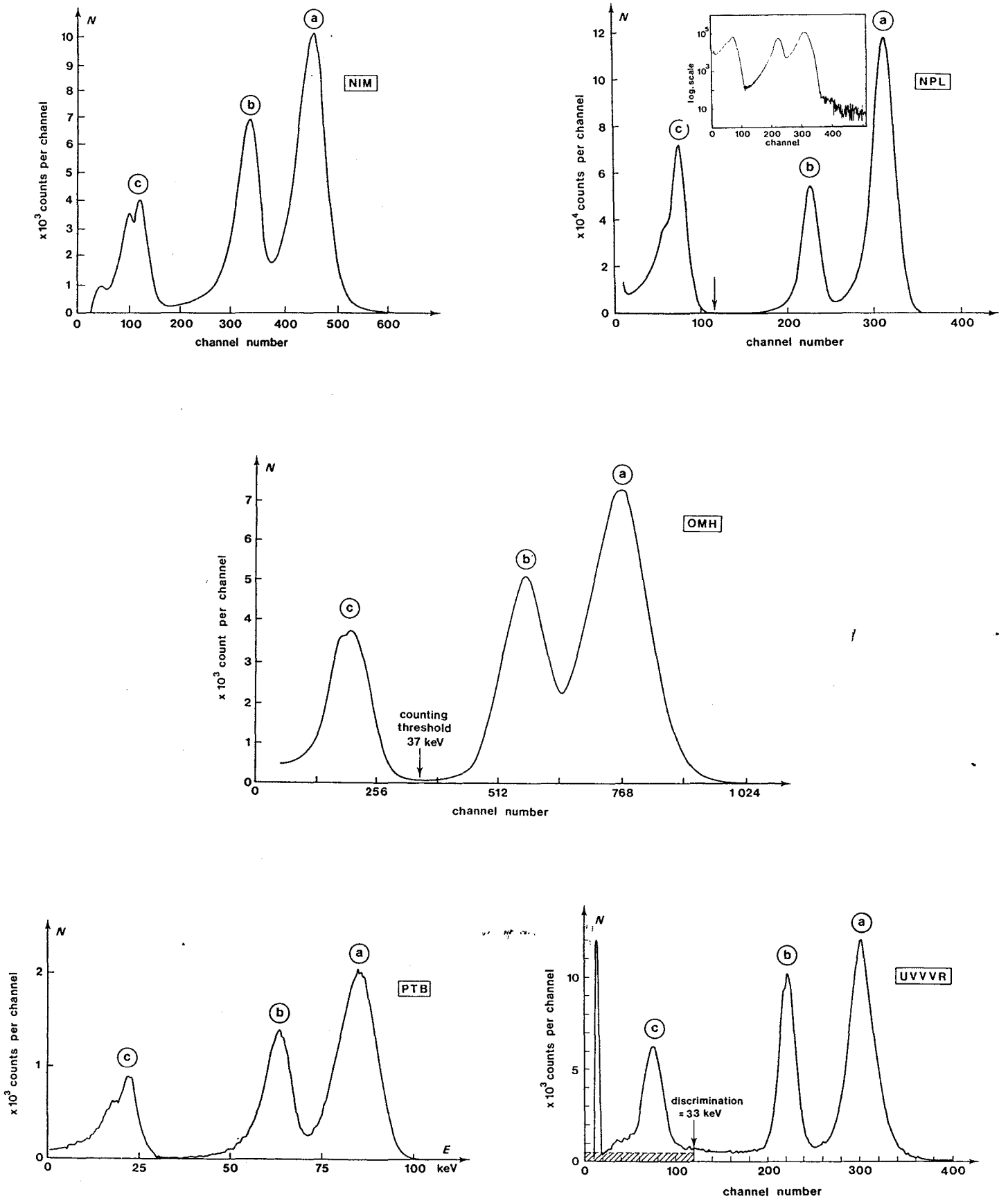


Fig. 2.1 (continued)

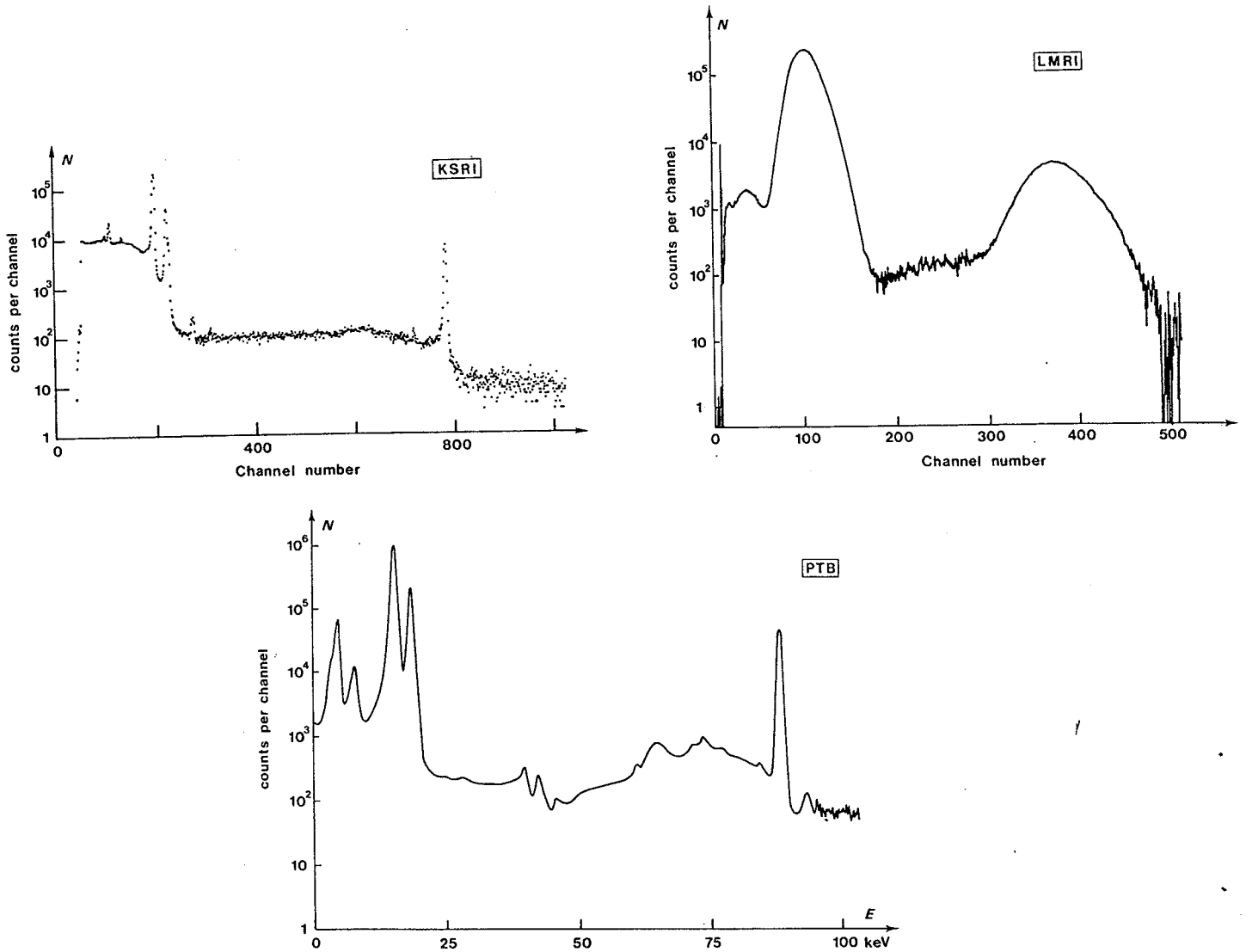


Fig. 2.2 - Typical photon spectra measured in order to obtain directly the 88 keV photon-emission rate.

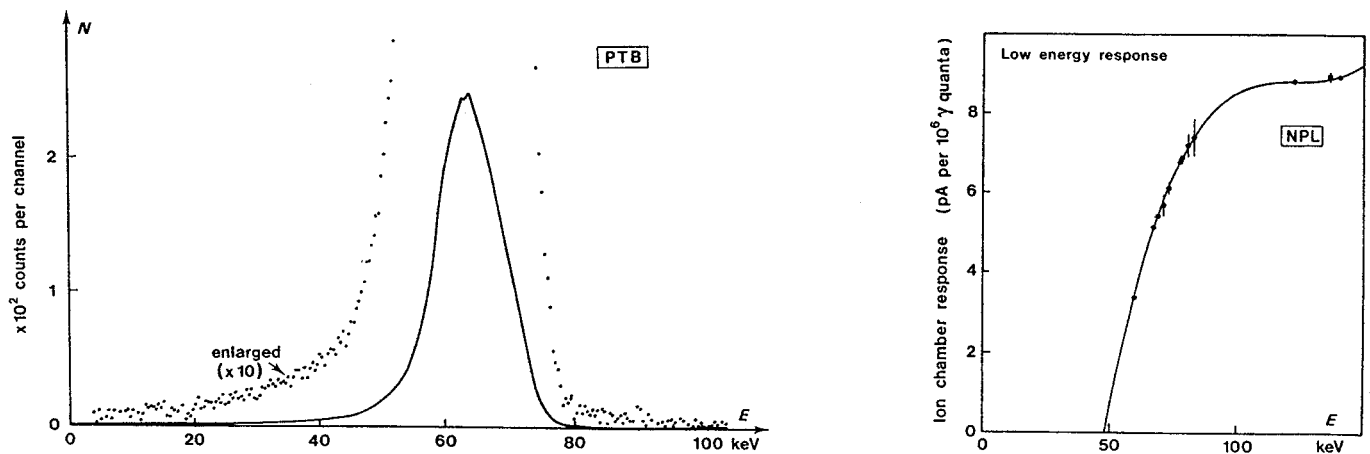


Fig. 2.3 - X-ray spectrum measured by means of a well-type NaI(Tl) detector surrounding the pressurized proportional counter (PTB).  
- Low-energy response of the ion chamber used by NPL to determine the 88 keV photon-emission rate.

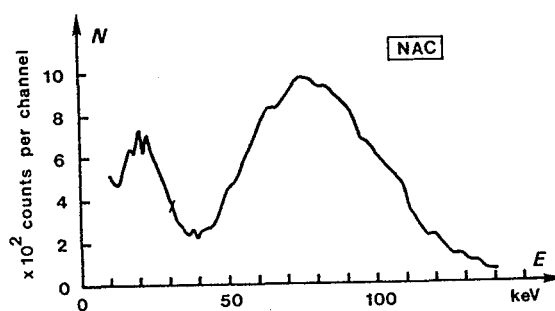
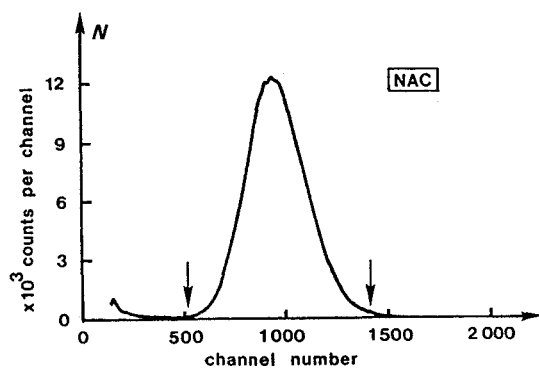
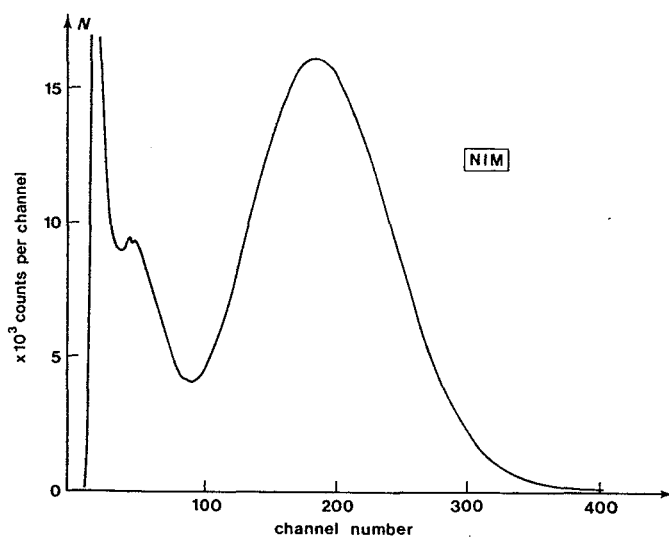
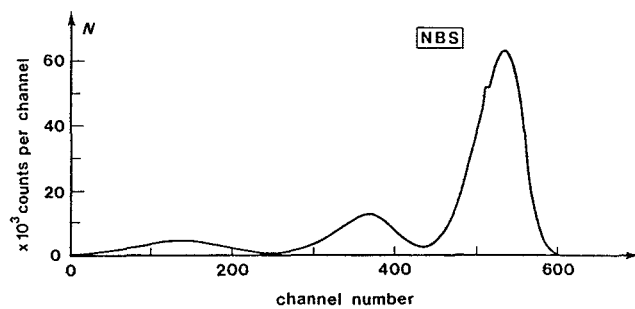
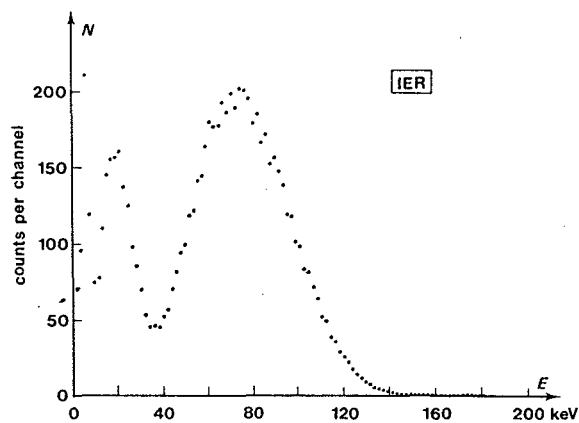


Fig. 3 - Typical conversion-electron spectra obtained by means of the liquid-scintillation method. The first NAC spectrum refers to 22 keV X rays measured with a thin  $\text{CaF}_2(\text{Eu})$  detector.

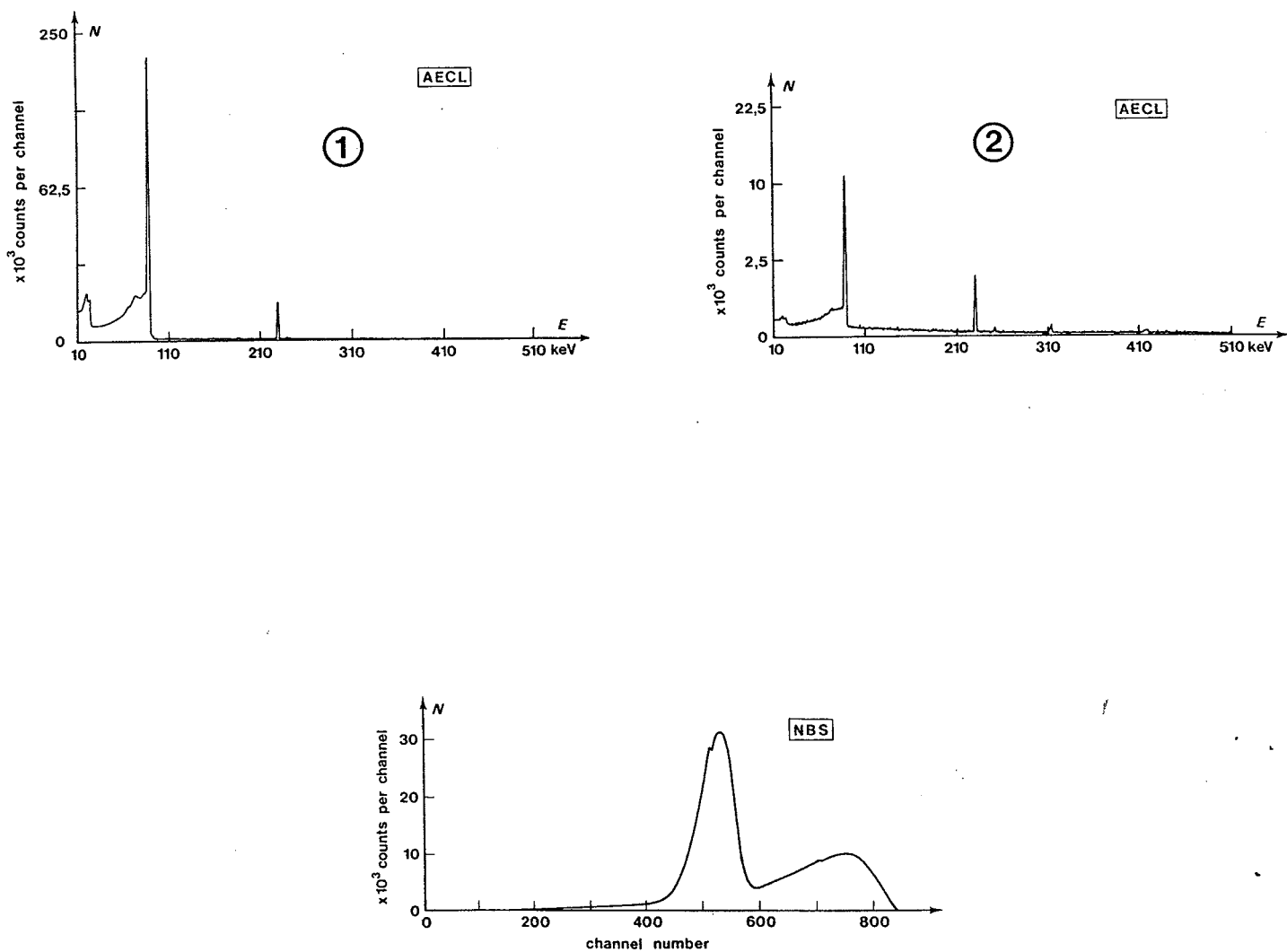


Fig. 4 - Typical spectra obtained by AECL and NBS when standardizing a  $^{109}\text{Cd}$  solution.  
 AECL uses a Ge(Li) detector to measure the  $\gamma$ -emission rate of the  $^{109}\text{Cd}$  spectrum (1) and the  $^{109}\text{Pd}$  spectrum (2). NBS uses the liquid-scintillation method to get a  $^{109}\text{Pd}$  spectrum.

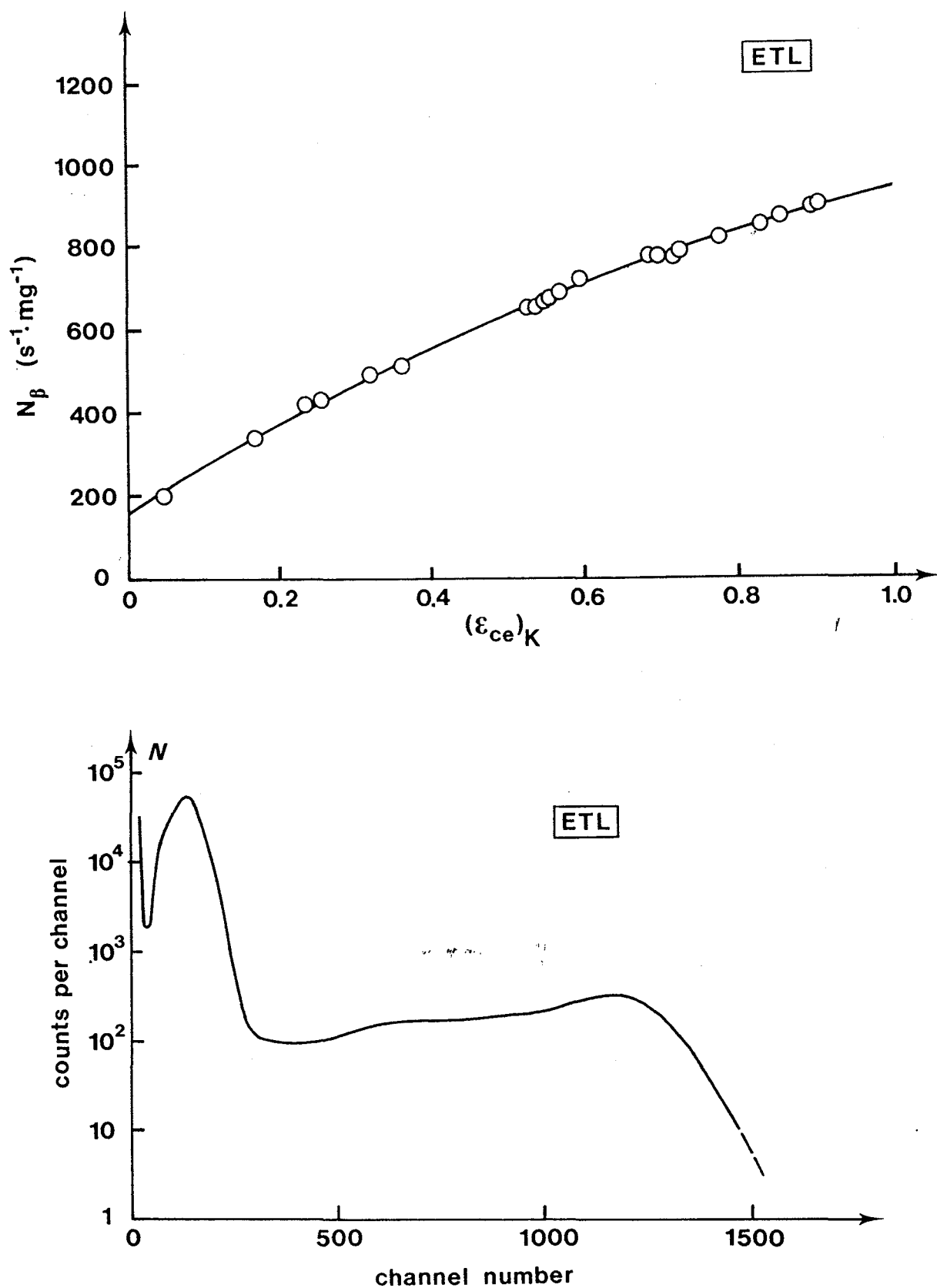


Fig. 5 - Typical curves obtained with the  $4\pi\epsilon$ -X coincidence method used by ETL. Upper part: behaviour of the  $\beta$  count rate versus efficiency  $(\epsilon_{ce})_K$ . Lower part:  $\gamma$ -ray spectrum from  $^{109}\text{Cd}$ .

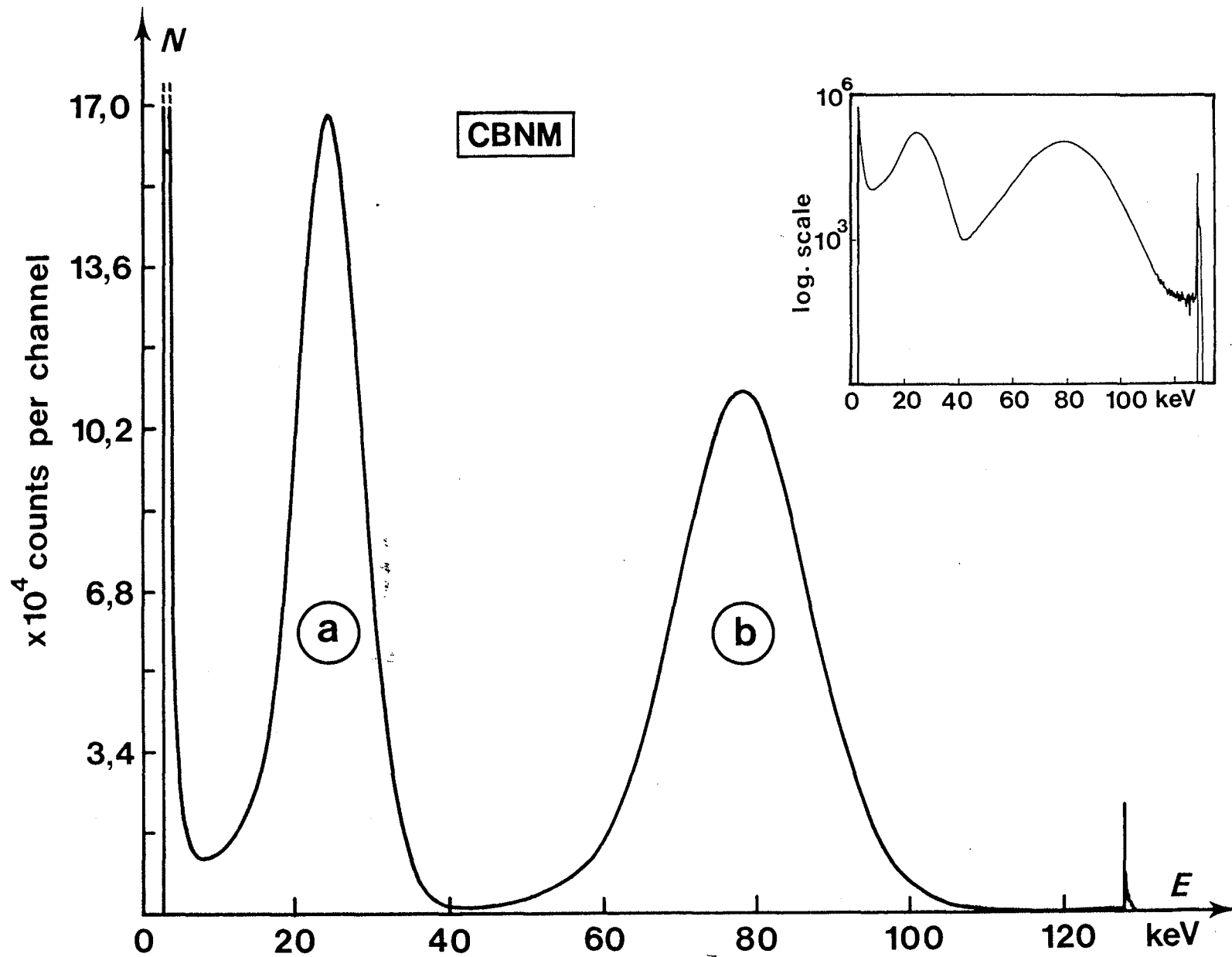


Fig. 6 - Typical spectrum from  $^{109}\text{Cd}$  obtained by means of a  $4\pi\text{CsI(Tl)}$  sandwich spectrometer.  
 (a) refers to K X-ray and K-Auger electrons, and (b) refers to K,L conversion electrons.



## References

- [1] J. Blachot, Nuclear Data Sheets for A = 109, Nucl. Data Sheets 41, 1984, p. 111
- [2] A. Szörényi, Report on a trial comparison of activity measurements of a solution of  $^{109}\text{Cd}$ , Rapport BIPM-85/10, 1985, 15 p.
- [3] G. Ratel and J.W. Müller, International comparison of activity measurements of a solution of  $^{109}\text{Cd}$ , Preliminary report, Rapport BIPM-86/13, 1986, 6 p.
- [4] K. Pochwalski, R. Broda, T. Radoszewski and P. Zelazny, Standardization of low-level beta-emitter solutions by using the liquid-scintillation triple to double coincidence ratio method, in International Symposium on methods of low-level counting and spectrometry, Berlin 1981, IAEA-SM-252/62
- [5] Y. Kawada, Extended applications and improvement of the  $4\pi\beta\text{-}\gamma$  coincidence method in the standardization of radionuclides, Res. of the ETL, n° 730, 1972, p. 66
- [6] R.H. Martin and J.G.V. Taylor, Standardization of  $^{109}\text{Cd}$  by  $4\pi\text{e-X}$  coincidence method, Proc. of ICRM Seminar, Rome, 1987, Appl. Radiat. Isot. A38, p. 781
- [7] J.S. Merritt, R.H. Martin and L.V. Smith, Standardization of  $^{109}\text{Cd}$ , in Progress report, Physics Division, 1982, PR-P-133, Atomic Energy of Canada Limited, Report AECL-7683
- [8] J.W. Müller, Dead-times problems, Nucl. Instr. and Methods 112, 1973, p. 47
- [9] M.E.C. Troughton, A method for measuring the nuclear transformation rate of  $^{109}\text{Cd}$ , Int. J. Appl. Rad. Isot. 28, 1977, p. 773
- [10] F. Lagoutine, N. Coursol, J. Legrand, Table des radionucléides, CEA-LMRI 1982
- [11] W. Bambynek, On selected problems in the field of proportional counters, Nucl. Instr. and Methods 112, 1973, p. 103
- [12] D.F.G. Reher, B. Denecke and R. Vaninbroukx, Standardization of a  $^{109}\text{Cd}$  solution, Report GE/R/RN/07/85, 1985
- [13] P. Giacomo, News from the BIPM, Metrologia 17, 1981, p. 69
- [14] H.H. Hansen, Evaluation of K-shell and total internal conversion coefficients for some selected nuclear transitions, European Applied Research Dept. Nucl. Ser. Technol. 6, 1985, pp. 777-816

- [15] A. Becker, J. Lamé, M. Vallée, Simulation d'interactions primaires de photons en milieu limité par un cylindre droit (IPPC), Rapport CEA-R-4498, Saclay
- [16] K. Rundt, H. Kouru, T. Oikari, Theoretical expressions for the counting efficiency and pulse height distribution obtained for a beta-emitting isotope by a liquid scintillation counter, in Proceedings of the Conference on advances in scintillation counting, Baniff, Canada, 1983
- [17] C. Ballaux and J.M.R. Hutchinson, Measurement of the gamma-ray emission rate of  $^{109}\text{Cd}$  with a well-type NaI(Tl) detector, Int. J. Appl. Rad. Isot. 37, 1986, p. 923

(September 1988)